**Exploring the long-term water quality of Waterhen Lake (Manitoba, Canada), an eco-certified fishery**

**by**

**Dawsyn Sturch**

**A thesis submitted to the Department of Biological Sciences, University of Manitoba, in partial fulfilment of the requirements for the course**

**BIOL 4100 (Honours Thesis)**

**for the degree of**

**Bachelor of Science (Honours)**

**©April, 2026**

**Abstract**

Waterhen Lake (Manitoba, Canada) is a large, shallow lake (272 $km^2$, maximum depth = 4.4 m) located in the highly understudied and undeveloped Boreal Plains Ecozone (BPE). BPE lakes are very sensitive to climate change and nutrient enrichment from relatively proximal agricultural land use. Waterhen Lake is a Marine Stewardship Council eco-certified fishery for walleye and northern pike, and an important commercial and sustenance fishery for surrounding Indigenous communities. However, no routine historical water quality monitoring had ever been done on the lake, leaving much about its ecosystem health unknown. Using two $^{210}$Pb-dated sediment cores, fossil pigment concentrations and diatom community composition were evaluated to determine changes in phytoplankton composition and abundance as a proxy for overall water quality over the last ~150 years. In the early 1900s, lake production was lower, and small, benthic fragilarioid diatoms were prominent. Phytoplankton production in Waterhen Lake then began to increase ca.1970–1980 concurrently with climate change associated increases in mean annual and winter temperatures. Increased production was indicated by higher pigment concentrations, shifts in phytoplankton community composition, and shifts in diatom community composition to increased abundances of planktonic taxa. Additionally, declines of nitrogen-fixing Nostocales cyanobacteria has likely resulted from nutrient enrichment (nitrogen) from upstream agricultural land use. These results indicate increased biological production has occurred in Waterhen Lake, signaling degraded water quality and aquatic health, and suggests that local fishers and managers should be prepared to adjust to changing conditions.

**Acknowledgements**

I would like to thank Dr. Cale Gushulak for providing invaluable support and guidance with my project. I would also like to thank Dr. Margaret Docker and Dr. Gail Davoren for providing helpful feedback and editing of my thesis.

I would like to thank Geoff Klein with the Province of Manitoba for assisting in core collection and providing the use of the snowmobiles and ice auger that were used to collect the cores. I would also like to thank Lorne, a local fisher for allowing us to use his property to access Waterhen Lake. I also thank Madeline Minor for her help with the LOI procedure on the sediment cores, Anthony Buckley with the Department of Soil Science for providing instruction and help with the $^{210}$Pb dating procedure, Claire Herbert with the Centre for Earth Observation Science for sharing Waterhen Lake water quality data, and Liam Numrich and Ryan Rimas at the University of Regina for their assistance in pigment analysis and interpretation. I would like to thank master's student Samadhi Jayathissa for her support.

Thank you to my family for providing support and reading my thesis and watching my presentations countless times.

Thank you to the University of Manitoba and NSERC for providing funding for my project.

I would like to acknowledge that the lab work done at the University of Manitoba took place on Treaty One lands the traditional lands of the Anishinaabeg, Ininiwak, Anisininewk, Dakota Oyate, Dene, and Dakota. Waterhen Lake is located on Treaty Two land the traditional lands of the Dakota Oyate and Anishinaabeg, and Treaty Five lands traditional lands of the Cree, Dene, and Inuit. Treaties One, Two, and Five lands are the Birthplace of the Métis Nation and Heart of the Métis Homeland.

**Contents**

**Abstract**.....i
**Acknowledgements**.....ii
**Introduction**.....1
**Methods**.....7
*Site description*.....7
*Sediment core collection*.....9
*Laboratory analysis*.....9
*Statistical analyses*.....13
**Results**.....15
*Dating*.....15
*LOI*.....15
*Pigments*.....16
*Core 1 – pigments*.....16
*Core 2 – pigments*.....17
*Diatoms*.....18
**Discussion**.....21
*Pigments*.....22
*Diatoms*.....31
*Food-web implications*.....34
**Conclusion**.....35
**Literature Cited**.....37
**Figures**.....61
**Tables**.....71
**Appendix A – Supplementary Tables**.....72
**Appendix B – Supplimentary Figures**.....73
**Appendix C – Core Data**.....80
**Appendix D – Calculations**.....85

**Figures**

Fig. 1. Boreal Plains Ecozone map ..... 61
Fig. 2. Waterhen Lake and core locations map ..... 62
Fig. 3. Bayesian age-depth model for core 1 ..... 63
Fig. 4. Bayesian age-depth model for core 2 ..... 64
Fig. 5. Algal pigment concentration data with CONISS test for core 1 ..... 65
Fig. 6. Chlorophyll a: pheophytin a ratio for core 1 ..... 66
Fig. 7. Algal pigment concentration data with CONISS test for core 2 ..... 67
Fig. 8. Chlorophyll a: pheophytin a ratio for core 2 ..... 68
Fig. 9. Diatom relative abundance data with CONISS test for core 1 ..... 69
Fig. 10. Diatom relative abundance PCA test for core 1 ..... 70

**Tables**

Table 1. Core collection information ..... 71

## Introduction

Lakes are important ecological, social, and economic resources; however, many are being substantially impacted by anthropogenic stressors, including climate change, nutrient pollution, and aquatic invasive species (Griffiths et al. 1991; Keller 2007; Schindler 2009; Nanayakkara 2018). Lakes located in the Canadian Boreal Plains Ecozone (BPE) (Fig. 1), a transitional zone between the heavily agricultural grasslands of the Canadian Prairies and deciduous and coniferous forested ecosystems of western Canada, are particularly sensitive to anthropogenic effects as they are exposed to the stressors affecting both prairie and boreal lakes (Hall et al. 1999; Keller 2007; Ireson et al. 2015; Nanayakkara 2018). Despite the vulnerability of BPE lakes, relatively little research has been conducted on the biogeochemical, biological production, and phytoplankton community responses to anthropogenic stressors, creating a critical gap in our understanding of BPE lake ecosystems, particularly in comparison to highly studied lake systems in the boreal region (e.g., the Experimental Lakes Area) (Malley and Mills 1992; Ireson et al. 2015).

Anthropogenic climate change is causing shifts in the biological, chemical, and physical properties of lakes worldwide (Schindler 2009; Tanentzap et al. 2020; Marty et al. 2021; Woolway et al. 2021). Higher water temperatures extend periods of thermal stratification in lakes, which can lead to hypolimnetic (lower most layer of water during stratification) anoxia, especially when paired with eutrophication; the process of excessive nutrient loading causing increased primary production (Portielje and Van der Molen 1999; Wetzel 2001; Beutel 2003; Chapra 2008; Winter et al. 2011; Welch et al. 2011; Foley et al. 2012; Qin et al. 2013; Null et al. 2017; Woolway et al. 2021; Devlin and Brodie 2023). During hypolimnetic anoxia, internal release of biologically available nutrients (e.g.,

phosphate and ammonium) from the sediments due to lowered redox potential can further increase biological production (Boström et al. 1988; Beutel 2006; Howarth et al. 2011; Cormier et al. 2023). Additionally, elevated biological production is often coupled with increased oxygen demand for the decomposition of the decaying algal biomass (Terry et al. 2017). Highly anoxic conditions can lead to fish kills if sustained (e.g., under ice), and even low-oxygen-tolerant fish species such as walleye (*Sander vitreus*) may become stressed under prolonged hypoxic or anoxic conditions (Barica and Mathias 1979; McMahon et al. 1984; Stewart et al. 2016; Raabe et al. 2020). In addition, habitat loss for cool-water adapted fish occurs as warm, surface water layers deepen due to prolonged warmer air temperatures (Gaeta et al. 2014; Hansen et al. 2019; Raabe et al. 2020). Further, climate change induced warming causes increased surface water temperatures creating favourable conditions in the epilimnion (upper most layer of water during stratification) for the proliferation of warm-adapted phytoplankton such as cyanobacteria, including species of cyanobacteria that produce harmful toxins (e.g., *Microcystis*) (Wetzel 2001; Foley et al. 2012; Thomas and Litchman 2016; Weber et al. 2020; Li et al. 2025).

Nutrient inputs (nitrogen and phosphorus) from widespread and long-term agriculture have increased biological production and incidences of harmful algal blooms in many lakes located across the prairie region (Waiser and Robarts 1997; Bunting et al. 2016; Morales-Marín et al. 2017; Gushulak et al. 2024). Eutrophication impacts the composition of phytoplankton communities in lakes, with high-nutrient tolerant taxa (e.g., cyanobacteria) becoming dominant (Dixit et al. 2000; McDonald and Lehman 2013; Bjorndahl et al. 2022; Gushulak et al. 2024). Further, eutrophication in lakes alters light conditions as high phytoplankton growth in surface waters occlude and refract light, which

may impact the entire food-web by decreasing macrophyte abundance, benthic primary production, and fish visual hunting ability (e.g., walleye) (Portielje and Van der Molen 1999; Wetzel 2001; Vadeboncoeur et al. 2003; Bayley et al. 2013; Hilt et al. 2013; Nieman et al. 2018).

Waterhen Lake, located in the BPE region of central Manitoba, is an important commercial fishery and an area for subsistence fishing for the Indigenous peoples of Skownan First Nation, located on the south shore of the lake (Ireson et al. 2015; Galbraith et al. 2017). Fish harvested from Waterhen Lake have a landed average value of $104,637 per year and a walleye harvest limit of 34.6 metric tonnes (Galbraith et al. 2017). Since 2003, Waterhen Lake has been stocked with 3.7 million walleye to achieve these harvest levels (Galbraith et al. 2017). Waterhen Lake is also certified by the Marine Stewardship Council as being an eco-certified sustainable fishery for walleye and northern pike (*Esox lucius*) (MSC 2014; Casselman et al. 2024). The stability of the fishery depends on the overall environmental health of the lake, making a holistic understanding of the ecosystem and water quality critical in making informed and sustainable management decisions (Raabe et al. 2020). However, no long-term water quality data from the lake are available, and local communities accessing the lake have expressed concern about degraded water quality and under-ice fish kills (MSC 2014; Galbraith et al. 2017; Casselman et al. 2024). In addition, studying Waterhen Lake provides a unique opportunity to look at the widespread effects of anthropogenic stressors on lake health of sensitive BPE lakes (Keller 2007; Ireson et al. 2015; Nanayakkara 2018).

In the absence of long-term water quality monitoring, paleolimnological techniques can be used to evaluate whole lake ecosystems through time, and to predict future

environmental conditions using past trends of various environmental proxies (Smol 2010; Watson and Medeiros 2021; Griffiths et al. 2022). Paleolimnological approaches allow for inference of ecological and climate conditions through the analysis of biological, geochemical, and biogeochemical markers preserved in sediment cores (Laird et al. 1996; Benoit and Rozan 2001; Laird and Cumming 2008; Griffiths et al. 2022; Gushulak et al. 2024). Phytoplankton markers preserved in lake sediments (i.e., fossil pigments and diatoms) are commonly used in paleolimnology to assess changes in phytoplankton communities through time (Sanger and Gorham 1970; Dixit et al. 1992; Leavitt and Hodgson 2001; Reavie et al. 2014; Burge et al. 2018). Studying phytoplankton in paleolimnology is useful as phytoplankton are sensitive to changes in environmental conditions (e.g., nutrients and temperature) and are at the base of aquatic food-webs (Dixit et al. 1992; Naselli-Flores and Padisák 2023).

Fossil pigments (chlorophylls and carotenoids) that are deposited in the sediment reflect the production and community composition of phytoplankton, macrophyte, and terrestrial plant growth surrounding a lake during a select period of time (Sanger and Gorham 1970; Leavitt and Hodgson 2001). However, the majority of pigments that are deposited into aquatic sediments originate from phytoplankton sources, and the type and concentration of pigments in each sediment sample can be used to infer community composition (Leavitt et al. 1989; McGowan et al. 2005). For example, the pigment myxoxanthophyll represents types of cyanobacteria that can form floating colonies, while chlorophyll b represents green algae (chlorophytes) (Leavitt 1993; Leavitt and Hodgson 2001). Some pigments, such as pheophytin a are universal throughout photosynthetic phytoplankton and indicate changes in total algal abundance (Leavitt and Hodgson 2001).

Changes in total algal abundance signify changes in whole lake production and overall water quality (Bunting et al. 2016; Bjorndahl et al. 2022). Additionally, changes in the community composition of pigment depositing organisms such as algae can infer changes in community composition at higher tropic levels (e.g., fish) (McGowan et al. 2005). The preservation of pigments depends on the type of pigment as well as the thickness of the anoxic layer in a lake during deposition (Sanger and Gorham 1970). Lakes with thick anoxic layers in the water column prevent oxidative degradation of pigments, resulting in more pigments being preserved in sediment (Sanger and Gorham 1970). Additionally, pigments may be degraded through bleaching due to photo-oxidation (Leavitt 1993). Photo-oxidation occurs during deposition, and pigments that originate closer to the water's surface and take longer periods of time to sink to the sediment tend to be most impacted (Leavitt 1993). Although there is potential for the degradation and loss of fossil pigments in the sediment record, fossil pigments have been used in numerous studies as a reliable metric to demonstrate changes in phytoplankton community composition and production and lake water quality through time (Sanger and Gorham 1970; Leavitt 1993; Dixit et al. 2000; Bunting et al. 2016; Reavie et al. 2017).

Diatoms are a group of single celled algae (class Bacillariophyceae) present in most types of waterbodies, that preserve well in aquatic sediments after deposition due to their siliceous cell walls (Dixit et al. 1992). Diatoms are highly diverse but identifiable by their complex morphology (Dixit et al. 1992). Further, many diatom taxa are associated with a narrow and specific range of environmental conditions, allowing species compositions to be used to evaluate historical changes in environmental conditions such as phosphorus levels and biological production (Dixit et al. 1992; Laird and Cumming 2008). Shifts in diatom

assemblages in lakes are also common indicators of climate change (Rühland et al. 2015). Changes in diatom assemblages from heavily silicified benthic taxa to long, thin, colonial planktonic taxa is a frequently an indicator of climate change associated alterations in lake ecosystems including changes in thermal stability, water level, and production (Moos et al. 2005; Heinsalu et al. 2008; Rühland et al. 2015; Liu et al. 2020). Additionally, changes in higher trophic levels (e.g., fish) are often reflected by shifts in diatom taxa and abundance (Dixit et al. 1992).

Sediment age-depth relationships are used to determine when any noted changes in ecosystem structure and function, as marked by biogeochemical and biological proxies, likely occurred (Appleby et al. 1986; Benoit and Rozan 2001; Griffiths et al. 2022). Sediment age-depth relationships also allow ecological changes to be linked to shifts in climate and land use records (Burge et al. 2018). Estimated dates can be assigned to sections of a core through measuring the activity of radioisotopes primarily as $^{210}$Pb (Appleby et al. 1986; Binford 1990). $^{210}$Pb is a $^{238}$U series radioisotope that occurs naturally; it is formed through the isotope $^{226}$Ra decaying to $^{222}$Rn, which can decay to form $^{210}$Pb within the sediment (Appleby and Oldfieldz 1983; Binford 1990). Since $^{222}$Rn is gaseous, some is released into the atmosphere, which decays into $^{210}$Pb, then atmospheric fallout deposits the $^{210}$Pb into aquatic sediments (Appleby and Oldfieldz 1983; Binford 1990). The $^{210}$Pb that is the result of atmospheric fallout is measured to assign dates to sediment (Appleby and Oldfieldz 1983). The half-life of $^{210}$Pb is 22.26 years and exponential declines in $^{210}$Pb activity with depth (in the absence of sediment disturbance) allow for the aging of sediment samples up to ~150 years age, and anthropogenic activities to be linked to changes in paleolimnological indicators (Robbins 1978; Robbins et al. 1978;

Binford et al. 1993; Pienitz et al. 2006; Bunting et al. 2016; Reavie et al. 2017; Bjorndahl et al. 2022). Reliable age-depth models are essential in paleolimnological studies to make accurate interpretations of past environmental conditions through time (Webster et al. 2025).

My honours thesis will examine how the biogeochemistry, overall biological production, and phytoplankton community composition of Waterhen Lake, as an example of other large fishery lakes in the BPE has changed through time. My project will address the lack of water quality data available for Waterhen Lake using paleolimnological proxies of algal community composition and production as markers of past overall water quality, and to infer possible impacts on higher trophic levels including the target species of the fishery. In addition, my project will add to the knowledge about the effects of climate change and other human-induced stressors on BPE lakes over time. I hypothesize the water quality of Waterhen Lake will have been degraded through time as marked by increased fossil pigment concentrations and changes in diatom assemblages that indicate increased growth due to anthropogenic stressors such as climate change, and upstream nutrient inputs that are likely negatively affecting the lake's fishery. I also predict a greater degree of changes in these algal proxies in more recent sediments, signifying increased anthropogenic stress on the environment in recent decades.

## Methods

### *Site description*

Waterhen Lake is a large (272 $km^2$) and shallow (maximum depth = 4.4 m) lake located in the BPE in central Manitoba. It receives inflow from Lake Winnipegosis via the West Waterhen and Little Waterhen rivers, and outflows into the north basin of Lake Manitoba

via the Waterhen River (Fig. 2) (Galbraith et al. 2017). Water chemistry parameters were measured for the first time in 2016 and 2017 by the Manitoba Great Lakes Program through the Centre for Earth Observational Science (University of Manitoba). These data were shared by the project lead C. Herbert (Appendix A, Table 1). The average total dissolved phosphorus (TDP) for the 2016 and 2017 data combined was 20.7 µg/L and the average chlorophyll a (chl a) was 1.89 µg/L. These metrics indicate that Waterhen Lake is mesotrophic (ECCC 2010; Zhao et al. 2023). Average total dissolved nitrogen (TDN) was 631 µg/L and the TDN: TDP ratio is ~30, indicating phosphorous limitation (Appendix A, Table 1) (Guildford and Hecky 2000; Friesen-Hughes et al. 2021). The input of water from Lake Winnipegosis likely contains nutrients originating from agricultural land in the southern portion of the Lake Winnipegosis catchment which has experienced substantial increases in fertilizer application over the last ~50–60 years (Statistics Canada 1961–2022; AAFC 2023). In contrast with upstream agricultural land use, the direct catchment of Waterhen Lake is largely boreal forest and wetlands with minimal human development (AAFC 2023). The geology surrounding Waterhen Lake consists of calcium-rich, reefal limestones, dolostones, and bituminous laminates of Devonian age (Province of Manitoba 2024).

The climate of the region is defined by short summer seasons, mean annual precipitation levels of 536 mm, mean annual temperatures of -0.1˚C, and snow cover that lasts for one third of the year (Ireson et al. 2015; ECCC 2025a, 2025b). Long-term (~1960–2023 for temperature, 1960–2017 for precipitation) precipitation and temperature data from Grand Rapids Manitoba (~100 km from Waterhen Lake) was used, since Grand Rapids has the closest weather station with historical data and is also located in the BPE (Ireson et al.

2015; ECCC 2025a, 2025b). Mean annual temperature and winter temperatures began increasing ca. 1975 and have increased by ~1˚C and ~5˚C respectively, on average (Appendix B, Figs. 1 and 2) (ECCC 2025b). Winter precipitation was elevated in the region ca. 1960–1970 (Appendix B, Fig. 3) (ECCC 2025a).

*Sediment core collection*

On March 25, 2025, I participated in the collection of two sediment cores (Table 1) using a Glew gravity corer (Glew 1989) from Waterhen Lake, Manitoba, in collaboration with the Province of Manitoba Department of Natural Resources and Indigenous Futures. Each of the sites were accessed by snowmobiling across the frozen lake to known, deep locations where sediment was most likely to deposit. An electric auger was used to drill a hole in the ice at each location to enable sediment collection. Each core was sealed in the tube and covered with a black garbage bag to prevent photodegradation of pigments. The cores were transported to the University of Manitoba and stored in the dark at 4˚C until extrusion on March 26 and 27. The cores were sectioned at 0.5-cm intervals using a modified Glew core extruder (Glew 1989) and stored in whirl-pack bags in the dark at 4˚C until analysis. The samples were initially prepared for biochemical analysis in a dark lab by calculating the wet weight of the sediment samples.

*Laboratory analysis*

During the fall of 2025, sediment cores were dated by measuring the activities of the radioisotope $^{210}$Pb in select sediment samples (core 1 N = 13, core 2 N = 10) using alpha spectroscopy in the Soil Sciences Department in the Faculty of Agriculture and Food Sciences at the University of Manitoba. A subset of samples that were not used for loss-on-ignition (LOI) or pigment analysis (too little sediment left after subsampling for these processes) were used for the dating process (Appendix C, Tables 1 and 2). More samples

were not analyzed due to time and cost constraints. Gamma spectroscopy was initially conducted on the samples (summer 2025), but many of the activity results were too low to be used in further analysis due to insufficient sediment quantities in each sample (Appleby et al. 1986; Binford 1990; Zaborska et al. 2007). As result, the dating was repeated using alpha spectroscopy, which is more sensitive and uses smaller quantities of sediment per sample, but is destructive (Zaborska et al. 2007). Alpha dating was completed using the modified methods of Eakins and Morrison (1978). To quantify the activity of $^{210}$Pb, $^{210}$Po and $^{209}$Po were directly measured by the alpha spectrometer and used to calculate $^{210}$Pb activity (Appendix D, Equation 1) (Eakins and Morrison 1978). To complete this process a $^{209}$Po tracer in 1.5N hydrochloric acid was added to 0.7–1.0 g freeze-dried sediment samples along with additional 6N hydrochloric acid and heated at 180˚C for three hours (Eakins and Morrison 1978). The resulting supernatant was then mixed with a solution of 50 mL of distilled water and 5 mL of 10% ascorbic acid, and a silver coin was added to the solution before being heated over night at 80˚C (Eakins and Morrison 1978). The next day the silver coins were removed from the solution, rinsed with distilled water and placed in the alpha ensemble where radioactivity was measured (Eakins and Morrison 1978). This process had to be repeated twice, as the alpha counter could only hold 16 samples per run. Resulting radioactivity measurements were used to create Bayesian age-depth models for the sediment cores in *rplum* (Aquino-Lopez et al. 2018).

Sediment samples were analysed (summer 2025, completed by Madeline Minor) using loss-on-ignition (LOI) to determine the amount of organic matter (OM) and carbonate content present in the sediment (Dean 1974; Heiri et al. 2001). During this process an average of ~4.0 g of wet sediment from alternating 0.5-cm samples (i.e., every 1.0 cm)

(Appendix C, Tables 1 and 2) were dried in a muffle furnace at 105˚C for 18–24 hours before being cooled and heated to 550˚C for 4 hours, and then to 950˚C for 2 hours (Dean 1974; Heiri et al. 2001). Sediments were weighed between each heat treatment and calculations were performed to determine the amount of water, organic matter, and carbonate in the sediment samples (Appendix D, Equations 2 and 3) (Dean 1974; Heiri et al. 2001).

Sub-samples of the same intervals used for LOI (core 1, N = 30; core 2, N = 17) (Appendix C, Tables 1 and 2) were shipped to the Institute of Environmental Change and Society (IECS) at the University of Regina in early June for algal and cyanobacterial pigment analyses. Pigment analysis was performed on freeze-dried samples using high performance liquid chromatography (HPLC) and the standard procedures outlined in Leavitt and Hodgson (2001). Fossil pigments were extracted from small (~25–100 mg) amounts of dry sediment in an 80:15:5 solution of HPLC-grade acetone, methanol, and water for 12–24 hours at -20˚C before being filtered using syringes equipped with 2-µm pore mesh (Leavitt and Hodgson 2001). The resulting extract solution was dried under $N_2$ gas evaporation and then resuspended using HPLC injection solution (Leavitt and Hodgson 2001). Pigments were quantified using an Agilent 1100 HPLC system with a photodiode array detector using Sudan II as an internal standard (Leavitt and Hodgson 2001). Resulting pigment concentrations were standardized to organic matter (OM) content determined through LOI and were expressed as nmol $g^{-1}$ OM. Pigments quantified in sediment samples include fucoxanthin (labile pigment associated with siliceous algae), diatoxanthin (diatoms), alloxanthin (cryptophytes), pheophytin b (green algae), echinenone (total cyanobacteria), canthaxanthin (Nostocales cyanobacteria), and myxoxanthophyll (colonial cyanobacteria)

(Leavitt and Hodgson 2001; Bjorndahl et al. 2022). Aphanizophyll (cyanobacteria) was detected in both cores, but the trends were highly variable, so the pigment was not included in this thesis (Leavitt and Hodgson 2001). In addition, pheophytin a, the derivative product of chlorophyll a, and β-carotene were used as markers of total algal abundance (Leavitt and Hodgson 2001; Bjorndahl et al. 2022). The pigments lutein (chlorophytes) and zeaxanthin (cyanobacteria) were co-eluted on this HPLC system and were interpreted together as markers of "bloom-forming taxa" (Leavitt and Hodgson 2001). Finally, the ratio of chlorophyll a to pheophytin a was calculated for each point as a proxy for pigment preservation environment (Leavitt 1993).

Diatom sample preparation began in September 2025. A small amount (0.2–0.3 g) of wet sediment from alternating samples from core 1 (Appendix C, Table 1) was digested in a 1:1 M nitric (265 mL) and sulfuric (235 mL) acid solution (solution was prepared the day prior to digestion) for eight hours in an 80˚C water bath, to digest organic matter in the samples (Battarbee et al. 2001). Samples were stirred every hour during this process (Battarbee et al. 2001). The resulting acidic solutions was neutralized to a pH of ~7 by aspirating the acidic supernatant and resuspending the solution in deionized water over ~11 days (Battarbee et al. 2001). Diatom slurries were plated in 0.2-mL aliquots to coverslips and dried at room temperature and on a low temperature on a slide warmer before being affixed to microscope slides using heated Naphrax (a toluene-based resin) (Battarbee et al. 2001). To complete this process, coverslips were prepared by adding 0.5 µL of prepared diatom slurries to a glass vial, then adding ~15 mL of water to dilute to solution (Battarbee et al. 2001). The first sample was applied to the coverslip and then 10 mL of solution was removed from the glass vial, and then 10 mL of fresh distilled water was added again

(Battarbee et al. 2001). This process was repeated twice more to create four concentrations (i.e., four coverslips) of diatoms for each of the 31 samples (i.e., four concentrations per sample) (Battarbee et al. 2001). Due to the confidence in the age-depth model of core 1 (Fig. 3) being limited to ~20 cm, I enumerated and identified diatoms on 11 slides within the first ~20 cm of the core (i.e., every 2 cm evaluate a 0.5-cm interval from 0.5–20.5 cm in depth). The slide with a concentration for each sediment sample that has ~5–6 diatoms visible per view on the microscope was used to count and identify diatom taxa. Diatoms were enumerated and identified at 1000x magnification using a Nikon Eclipse NiL upright microscope with a 1.3 fluotar objective, oil condenser, and differential interference contrast. Each diatom was identified to species level whenever possible using available published and online resources (Krammer and Lange-Bertalot 1986; Krammer and Lange-Bertalot 1988; Krammer and Lange-Bertalot 1991a; Krammer and Lange-Bertalot 1991b; Spaulding et al. 2021), including a guide of prairie diatoms created by Dr. Kate Laird (Queen's University). Approximately 400 diatom valves were enumerated per slide.

*Statistical analyses*

The statistical tests were used to evaluate the response variables of phytoplankton pigment concentration and diatom taxa, over time. All statistical analysis and plotting were completed using R software (R Core Team 2025). Plots were made using *ggplot2* version 4.0.0*, ggfortify* version 0.4.19*, cowplot* version 1.2.0*,* and *plotly* version 4.11.0 while *tidyr* version 1.3.1, *tidypaleo* version 0.1.4, and *dplyr* version 1.1.4 were used for data management (Tang et al. 2016; Wickham 2019; Sievert 2020; Dunnington et al. 2022; Wickham et al. 2023, 2024; Wilke 2025). Bayesian age-depth plots from resultant $^{210}$Pb activity were created using *rplum* version 1.0.0 (Aqunino-Lopez et al. 2018). In addition to the values for $^{210}$Pb activity, $^{226}$Ra values from the deepest sediment intervals that

underwent the dating process in each core were needed to determine background $^{210}$Pb activity in order to use *rplum* (Aqunino-Lopez et al. 2018). Even though gamma spectroscopy did not produce overall usable results, $^{226}$Ra values from the three deepest intervals of core 1 that underwent gamma spectroscopy were used to create Bayesian age-depth model in *rplum* for core 1 (Aqunino-Lopez et al. 2018). There were not $^{226}$Ra values available for core 2, so the deepest sediment interval dated (17.5–18.0 cm) was used to set the background $^{210}$Pb activity. Dates found using the age-depth model were assigned to the sediment intervals in the cores used for pigment, LOI, and diatom analysis. Age-depth relationships for sediment intervals that were not dated directly were interpolated using *tidypaleo* (Dunnington et al. 2022). The confidence in the age-depth model was limited to ~20 cm in depth core 1, so plotting and statistical analyses of LOI, pigment concentrations, and diatom relative abundance values were limited to sediment intervals that fell within this depth (Appendix B, Table 1). Standardized pigment concentrations from each core were analyzed in Constrained Increment Sum of Squares (CONISS) cluster tests (Juggins 2024) using the *rioja* version 1.0.7 package (Juggins 2024). Fucoxanthin concentrations were not included in the CONISS test because of its high lability (Leavitt and Hodgson 2001). CONISS tests are multivariate analysis that produce hierarchical dendrograms by clustering similar groups of data together, while maintaining a chronology (allows for changes over time to be observed) (Grimm 1987). A broken-stick model was created in *rioja* to validate the number of significant clusters delineated in each CONISS dendrogram (Juggins 2024).

Diatom data were reduced to include only the most common taxa (a minimum of 5% abundance in at least two samples for plotting, a minimum of 1% relative abundance

in at least two samples for statistics). Principal Component Analysis (PCA) was conducted on the 1% relative abundance diatom data using *cluster* version 2.1.8.1 (Maechler et al. 2025). PCAs are used in paleolimnology to simplify large multivariate datasets (e.g., diverse diatom assemblage data) to determine directional shifts in community composition through time series (Jolliffe and Cadima 2016; Hu et al. 2023). Diatom 1% relative abundance data were Hellinger transformed (square-roots of proportional abundance values) to reduce skew in the multivariate data (Legendre and Borcard 2018). Following PCA analysis, a CONISS test was also performed on 1% diatom taxa data to evaluate when environmental changes occurred in time, since diatom taxa have specific environmental tolerances (Dixit et al. 1992).

## Results

### *Dating*

Bayesian age-depth models demonstrate a decaying curve exponential relationship in each core (Figs. 3 and 4). $^{210}$Pb activity measured with confidence to 18.5 cm in core 1 (Fig. 3) and 16.0 cm in core 2 (Fig. 4), corresponding to ~1900 in each core. Additionally, the accumulation rate of sediment was 11 years/cm and the accumulation rate of $^{210}$Pb 50 Bq/yr in both cores (Figs. 3 and 4).

### *LOI*

Carbonate content in both sediment cores was highest at ~1900 and then decreased in more recent sediment (Appendix B, Figs. 4 and 5). In both sediment cores, organic matter increased from ~1900–2025.

*Pigments*

*Core 1 – pigments*

The CONISS test for core 1 (Fig. 5) validated with a broken stick model (Appendix B, Fig. 6) produced a dendrogram with two significant groupings (group one = 1894–1974, group two = 1974–2025).

The rapid decline in fucoxanthin (Fig. 5) represented its degradation in the sediment due to its lability (Leavitt 1993; Leavitt and Hodgson 2001). Therefore, it was not interpreted ecologically in this thesis. Diatom concentrations (as diatoxanthin) were highest in group one but declined through time (Fig. 5). Concentrations of pigments reflecting cryptophytes (alloxanthin), green algae (pheophytin b), total cyanobacteria (echinenone), and total algal abundance (pheophytin a) remained low throughout majority of the group one but began to increase ca. 1960–1970 (Fig. 5). Concentrations of these pigments then declined briefly ca. 1980 (second grouping), before increasing again late ca. 1980 and continuing to increase throughout the 1990s and 2000s (Fig. 5). An overall increasing trend in total algal abundance (pheophytin a) was consistent with increases in organic matter (Fig. 5, Appendix B Fig. 4). Concentrations of β-carotene increased ca. 1900 and ca. 1970 (group one) and then exhibited considerable variability throughout the remainder of the sediment record (Fig. 5). Cryptophytes and green algae pigment concentrations exhibited a declining trend initiating ca. 2020, while total cyanobacteria (echinenone) pigment concentration exhibited an ~2-fold increase ca. 2020 (Fig. 5). Potentially nitrogen-fixing Nostocales cyanobacteria (canthaxanthin) fluctuated throughout the early 1900s, until a decline ca. 1960 (group one) (Fig. 5). Nostocales cyanobacteria then increased briefly ca. 1980 (group two), before a steady decline and overall ~2-fold decrease throughout the remainder of the 1900s and into the 2000s (Fig.

5). Bloom-forming taxa (lutein-zeaxanthin, representing green algae and cyanobacteria) increased throughout the early 1900s and reached the maximum concentration (group one) ca. 1925. This biomarker then declined ca. 1930–1960 before fluctuating throughout the second group and then declining to a minimum concentration ca. 2025 (Fig. 5). Colonial cyanobacteria (myxoxanthophyll) fluctuated considerably throughout group one (Fig. 5). Colonial cyanobacteria then remained elevated throughout majority of the second group, before beginning to decline ca. 2005 (Fig. 5).

The chlorophyll a: pheophytin a ratio was below 0.5 throughout the 1900s, until an increasing trend initiated ca. 1980 (Fig. 6). There was a brief peak in the ratio ca. 2005 at a ratio of ~2, and a rapid increase to a ratio above 3 ca. 2025 (Fig. 6).

*Core 2 – pigments*

The CONISS test for core 2 (Fig. 7) validated with a broken stick model (Appendix B, Fig. 7) produced a dendrogram with two significant groups (group one = 1893–1978, group two = 1978–2025).

Fucoxanthin also exhibited a degradation curve in core 2 (Fig. 7). In the first group, the majority of pigment concentrations ca. 1893–1978 (excluding bloom-forming taxa (lutein-zeaxanthin) and pigments associated with Nostocales (canthaxanthin) and colonial cyanobacteria (myxoxanthophyll)) were relatively stable (Fig. 7). All pigment concentrations (excluding cyanobacteria as echinenone) experienced consistent decreases in concentrations between the 1950s and 1970s (Fig. 7). In the second group of data, diatoms (diatoxanthin), cryptophytes (alloxanthin), green algae (pheophytin b), and total algal abundance (both β-carotene and pheophytin a) all showed an increase in pigment concentration leading up to and/or into the beginning of the second group in the data ca.

1980 (Fig. 7). Between the 1970s and 2000s there was a 1.4-fold increase in bloom-forming taxa (Fig. 7). The majority of cyanobacteria pigment concentrations (as canthaxanthin, and myxoxanthophyll) exhibited a declining trend throughout the first group (Fig. 7). Total cyanobacteria (echinenone) remained low throughout both groups with the two elevated points that are suspected outliers (Fig. 7). Nostocales cyanobacteria pigments declined ca. 1900–1970 (Fig. 7). This trend was continued in the second grouping of Nostocales cyanobacteria pigment concentrations, excluding and brief increase ca. 1970–1985 (Fig. 7). Colonial cyanobacteria pigments declined ca. 1940–1960 and then increased in the second group, but not until ca. 1990 (Fig. 7). Overall, pigment concentrations showed increasing concentrations since the 1960s–1970s (Fig. 7). The same trend was observed in the overall organic matter content of the sediment (Appendix B, Fig. 5).

The chlorophyll a: pheophytin a ratio fluctuated above and below a value of 0.5 throughout the early 1900s aside from one elevated data point ca. 1925 (Fig. 8). The chlorophyll a: pheophytin a ratio demonstrated a greater increasing trend after ~1975 (Fig. 8). Between ca. 2025 and ca. 2000, the chlorophyll a: pheophytin a ratio decreased from ~1.5 to ~1.0 (Fig. 8).

*Diatoms*

A total of 494 different taxa (primarily species level or lower) were identified from core 1. Diatom taxa generally consisted of high abundances of highly diverse, primarily benthic fragilairiod taxa such as *Pseudosturosira brevistriata* and *Staurosirella pinnata*. However, the benthic: planktonic ratio demonstrated a trend of increasing planktonic abundance

(i.e., lower benthic: plankton ratio values) in recent sediment samples (i.e., ~1975–present) (Fig. 9).

The CONISS test for the 1% relative abundance (Fig. 9) validated with a broken stick model (Appendix B, Fig. 8) produced a dendrogram with five significant groups (group one = 1892–1900, group two = 1900–1963, group three = 1963–1975, group four = 1975–2023, group five = 2023–2025). Based on the hierarchy of the groups in the CONISS test, groups four and five are being considered as the primary groupings and groups one, two, and three are being considered as secondary groupings (Grimm 1987). The CONISS test dendrogram plotted with the 5% relative abundance data showed that during the first group (1892–1900), benthic taxa including small benthic fragilarioids *Pseudostaurosira brevistriata*, *Staurosirella pinnata*, and *Staurosira construens*, as well as naviculoids such as *Amphora pediculus*, and *Nitzschia* species were elevated (Fig. 9). *Pseudostaurosira brevistriata*, *Staurosirella pinnata*, other pennate benthic taxa (group of diverse benthic taxa) had the high relative abundance (~20–25% relative abundance in each taxon) in the first group (Fig. 9). This trend continued into group two ca. 1900, where *Pseudostaurosira brevistriata*, *Staurosirella pinnata*, other pennate benthic taxa, and the benthic: plankton ratio remained high (Fig. 9). *Staurosira construens* and *Staurosirella pinnata* briefly declined ca. 1945–1955, before increasing again ca. 1960 (Fig. 9). *Amphora pediculus*, *Gomphonema* species, *Navicula* species all increased ca. 1945–1955 before declining ca. 1960 (Fig. 9). Additionally, other centric planktonic taxa, which included *Cyclotella*, *Aulacoseira*, and *Stephanodiscus* species, increased in concentration at the beginning of group two (ca. 1900–1910), then remained at relatively constant concentration throughout majority of group two (ca. 1910–1955) before

beginning to decline ca. 1960 (Fig. 9). In the third group, *Pseudostaurosira brevistriata*, *Staurosirella pinnata*, *Nitzschia* species, and the benthic: plankton ratio all declined ca. 1970, while planktonic *Fragilaria* taxa, other centric planktonic taxa, *Staurosira construens*, *Amphora pediculus*, *Gomphonema* species, and *Navicula* species all increased (Fig. 9). Other pennate benthic taxa abundances remained high throughout the third group (Fig. 9). In the fourth group, there were declines of benthic taxa such as small fragilarioids (*Pseudostaurosira brevistriata* and *Staurosirella pinnata* ca. 1975–1980, *Staurosira construens* ca. 1985–2005) (Fig. 9). *Amphora pediculus* and the benthic: plankton ratio both declined in the beginning of the fourth group (*Amphora pediculus* ca. 1985–2005, benthic: plankton ratio ca. 1975–1980) before remaining constant at lower values for the remainder of the group (Fig. 9). In parallel to the decline in benthic taxa, planktonic *Fragilaria* and centric plankton abundances increased and generally remained elevated throughout the fourth group (Fig. 9). Other pennate planktonic taxa fluctuated throughout the fourth group. In the fifth group (2023–2025), planktonic taxa continued to increase in abundances through increases in plankton *Fragilaria* and other pennate plankton taxa (including stellate colony-forming *Astrionella* species) (Fig. 9). In the fifth group there were also increases in *Gomphonema*, *Navicula*, and *Nitzschia* species while small fragilarioids, the benthic: plankton ratio, and other centric plankton taxa decreased (Fig. 9).

The PCA of diatom taxa at least 1% relative abundance showed a total of 48.9% of variance in diatom taxa was accounted for by the first (PC1) and second (PC2) principal components (Fig. 10). PC1 accounted for 26.5% of the variance in diatom taxa and PC2 accounted for 22.4% of the variance in diatom taxa (Fig. 10). Small, benthic fragilairiod

species are closely associated with one another (e.g., *Pseudostaurosira brevistriata*, *Staurosirella pinnata* varieties, *Staurosira construens*), with other small benthic taxa (e.g., *Amphora pediculus*), and heavily silicified centric taxa (e.g., *Aulacoseira* species, *Stephanodiscus* species) (Fig. 10). Conversely, longer pennate taxa such as *Nitzschia* species and plankton *Fragilaria* (e.g., *Fragilaria nanana, Fragilaria tenera*) are closely associated with each other and less associated with small, benthic diatoms (Fig. 10). In relation to the five CONISS groups, the clusters of data points in the PCA were not consistently organized. The clusters of data points (dates) in the PCA were generally divided into two groups (Fig. 10). The majority of data points from 1892–1970 were clustered together in one group and closely associated with small benthic fragilarioids such as *Pseudostaurosira brevistriata* (Fig. 10). While data points from 1980–2022 were generally clustered together into a second group and associated with some benthic taxa but more closely associated with planktonic taxa than the earlier data points (Fig. 10). The most recent data point from 2024 was located in isolation from the other points and associated with different taxa and higher abundances of planktonic *Fragilaria* and other pennate plankton taxa (Fig. 10).

**Discussion**

Waterhen Lake has become more productive throughout the past ~50 years, with major environment changes initiating ca. 1970–1980 (Figs. 5 and 7), coinciding with increases in mean annual temperature and winter temperature in the region (Appendix B, Figs. 1 and 2) (ECCC 2025b). Increased production is marked by elevated overall algal abundance and shifts in algal community composition (Figs. 5 and 7). Declines in Nostocales cyanobacteria paired with increases in other taxa such as cryptophytes, green algae, and colonial cyanobacteria indicate upstream agriculture is likely responsible for increased nitrogen

availability, driving these changes in community composition (Figs. 5 and 7) (Statistics Canada 1961–2022; Schindler et al. 2008; Blais et al. 2012). Additionally, shifts in diatom community composition showing increases in the abundances of planktonic taxa also indicate that climate change has altered thermal stability (Rühland et al. 2015; Liu et al. 2020). Together, these changes have likely affected light penetration within the water column causing a further shift in planktonic vs benthic production (Rühland et al. 2015; Liu et al. 2020). Fishery health in Waterhen Lake is likely being impacted by degraded water quality, and results of this study suggest that as climate change continues to impact the lake, water quality and fishery health will continue to deteriorate in the future (Barica and Mathias 1979; McMahon et al. 1984; Stewart et al. 2016; Raabe et al. 2020).

*Pigments*

Increases in total algal abundance initiating ca. 1970–1980 indicate that Waterhen Lake has become more productive in the last ~40–50 years (Figs. 5 and 7). Increases in total algal abundance in core 1 is primarily through increased green algae (pheophytin b) since the trends in green algae most closely match the trends in pheophytin a, although colonial cyanobacteria (myxoxanthophyll), and cryptophytes (alloxanthin) are also contributing (Fig. 5). In core 2, increases in total algal abundance are primarily through increases in diatoms (diatoxanthin) and cryptophytes (most closely match the trends in pheophytin a), although green algae and colonial cyanobacteria are also contributing (Fig. 7). While increases in algal production in prairie lakes have been tied to agricultural development, Waterhen Lake is not directly exposed to agricultural input (Bayley et al. 2013; Bunting et al. 2016; AAFC 2023). Agricultural land is far upstream of the lake and agricultural nutrients must pass through Lake Winnipegosis which likely retains a large amount of those nutrients (Donald et al. 2015; AAFC 2023). Instead, significant changes in algal

production and community composition in Waterhen Lake appear to align temporally with changes in regional climate conditions (Figs. 5 and 7; Appendix B, Figs. 1 and 2) (AAFC 2023; ECCC 2025b). Since the 1980s, there has been a global increase in phytoplankton production in lakes, which has been partly associated with warming temperatures due to climate change and allowed increased phytoplankton growth to occur in lakes that are relatively low in nutrients (Ho et al. 2019; Reinl et al. 2021). Waterhen Lake may be one of these historically low nutrient lakes that have become more productive due to climate change, since the lake is presently mesotrophic (20.7 µg/L mean TDP and 1.89 µg/L chl a 2016/2017; Appendix A, Table 1) (ECCC 2010; Reinl et al. 2021; Griffiths et al. 2022; Zhao et al. 2023). Additionally, the trophic status of Waterhen Lake indicates that agricultural nutrient inputs are not responsible for the increased phytoplankton production, as it would be expected that Waterhen Lake would presently be in a eutrophic or hypereutrophic state with much higher nutrient levels and changes in pigment production (Bunting et al. 2016; Griffiths et al. 2022). In the Waterhen Lake region, mean annual temperatures have increased by ~1˚C on average since the 1970s/1980s, mostly due to increased winter temperatures of ~5˚C on average (Appendix B, Figs. 1 and 2) (ECCC 2025b). Additionally, the variability of mean annual temperatures has also increased since the 1970s/1980s after which there are frequent occurrences of hot years where annual temperatures are ~2˚C above the average (Appendix B, Fig. 1) (ECCC 2025b). Further, these temperature increases are likely shortening the period of ice cover and lengthening the growing season which may also be contributing to increased algal abundance in Waterhen Lake, as phytoplankton blooms have appeared later in the year in other lakes as result of the longer growing season (Winter et al. 2011; Li et al. 2022; ECCC 2025b). This issue is likely to get worse, as shallow lakes in the northern

hemisphere have an estimated period of 10–25 days less ice cover per year in the future (Brown and Duguay 2011).

The increase in phytoplankton that Waterhen Lake began experiencing ca. 1970–1980 (Figs. 5 and 7) is also likely due to the internal nutrient loading of phosphorous, which is a process that often occurs in lakes with higher primary productivity (Tammeorg et al. 2020). Since Waterhen Lake is shallow (maximum depth = 4.4 m), it is likely not remaining stratified for long periods of time, but some studies have shown that anoxia at the sediment-water interface and the release of nutrients stored in the sediment commonly occur during the summer months in large and shallow lakes (Søndergaard et al. 2013; Nürnberg and LaZerte 2016; Galbraith et al. 2017). In addition, broad, shallow lakes like Waterhen Lake have a high sediment surface area to volume of water ratio, which increases the transfer of nutrient out of the sediment into the water during anoxia or due to wind mixing (Nürnberg and LaZerte 2016). Wind causes the full volume of water in a shallow lake to mix, dispersing nutrients throughout the water column and increasing nutrient availability for phytoplankton (Søndergaard et al. 2013; Nürnberg and LaZerte 2016). Wind-driven release of sedimentary nutrients is likely occurring in Waterhen Lake due to strong regional wind patterns (Ma et al. 2025).

Cyanobacteria production (as echinenone) has increased greatly ca. 2020 onwards in core 1 (Fig. 5). The increase in cyanobacteria (as echinenone) may also indicate that temperatures and nutrient levels within Waterhen Lake have increased further in recent years, since cyanobacteria thrive in warm, nutrient rich conditions (Wagner and Adrian 2009; Thomas and Litchman 2016). Although cyanobacteria as echinenone have increased in core 1, cyanobacteria as echinenone remained at constant low level throughout the

whole of core 2 excluding the two points that are suspected to be outliers (Fig. 7). This may be the result of depositional differences between the two sampling locations (Leavitt 1993; Leavitt and Hodgson 2001).

Concern has also been expressed by local communities accessing Waterhen Lake about under-ice fish kills. Under-ice fish kills are usually due to prolonged under-ice anoxia (Barica and Mathias 1979). In Waterhen Lake, the increased production (Figs. 5 and 7) is likely contributing to the under-ice fish kills in the lake (Terry et al. 2017). Mixing of the water in the fall prior to freezing introduces oxygen into the water, but once thick ice forms on the lake surface (>80-cm thick in Waterhen Lake, Table 1), the wind can no longer mix the water (Yang et al. 2020; Zhang et al. 2024). The lack of mixing and oxygen demand for decomposition causes the dissolved oxygen content in the lake to decline over the duration of the ice coverage period until the ice melts in spring (Terry et al. 2017; Zhang et al. 2024). Under-ice oxygen levels in shallow arctic lakes have been found to decline to as low as 20% of the oxygen that was present at the beginning of the winter season (Schwefel et al. 2023). In addition to decreasing oxygen content and increasing carbon dioxide in the lake, anoxia can increase the production of methane via methanogenesis, which can be released to the atmosphere when the ice melts in the spring (Gorsky et al. 2024; Bastviken and Johnson 2025). When the cores were extracted from Waterhen Lake and the sediment was being sectioned, a strong sulfur smell was noticeable. This smell was likely caused by $H_2S$ gas, which is a byproduct associated with methane production, indicating that there is methane production occurring under the ice in Waterhen Lake (Woszczyk et al. 2025). The release of these greenhouse gases (carbon dioxide and methane) creates a feedback cycle that exacerbates climate change effects

(Gorsky et al. 2024; Bastviken and Johnson 2025). It has been estimated that globally lakes release ~10% of the world's methane emissions, a number that is projected to increase with climate change (Bastviken and Johnson 2025). Although methane was not measured in this study, it is probable that Waterhen Lake has increased methane emissions because there has been increased algal production (Figs. 5 and 7) (Terry et al. 2017; Gorsky et al. 2024; Bastviken and Johnson 2025).

Across algae and cyanobacterial groups, pigment concentrations generally declined between ~1950 and ~1970 in core 2 (Fig. 7), although this trend was not observed in core 1 (Fig. 5). A large amount of Waterhen Lake's catchment is comprised of wetlands, which are known to be major sources of dissolved organic carbon to lakes (Hall et al. 2021; AAFC 2023). Additionally, snowmelt is known to wash dissolved organic carbon into lakes (Meingast et al. 2020). An increase in winter precipitation in the Waterhen Lake region in the 1960s and 1970s (precipitation data only goes back to the 1960s; Appendix B, Fig. 3) likely resulted in increased melt water flowing through wetland areas in the catchment causing increased organic carbon to enter the lake (Meingast et al. 2020; Hall et al. 2021). Increases in dissolved organic carbon may have limited planktonic, but likely primarily benthic growth in shallow waters during this period (Carpenter et al. 1998; Fork et al. 2020). At high concentrations, organic carbon can limit light availability and cause a decline in benthic production (Fork et al. 2020; Horppila et al. 2023). Additionally, the carbonate content in Waterhen Lake has decreased over time (Appendix B, Figs. 4 and 5) indicating that the dissolved organic carbon increased, because as dissolved organic carbon is decomposed, increased carbon dioxide in the water column causes carbonate material to decline through conversion to carbon

dioxide (Dean 1999). Evaluation of sediment $\delta^{13}C$ isotope values in future work will aid in determining if organic carbon deposition is elevated during this period of time and if the carbon is originating from a terrestrial, likely wetland, source (Pace et al. 2004; Hall et al. 2021).

In both cores Nostocales cyanobacteria (canthaxanthin) pigment concentrations show an overall declining trend through time (Figs. 5 and 7), which is the opposite of the majority of the other pigment concentration in both cores. This trend is likely because many Nostocales cyanobacteria are able to fix nitrogen and are competitively dominant under nitrogen limitation (Blais et al. 2012; Grover et al. 2022). Therefore, declines in Nostocales cyanobacteria (as canthaxanthin; Figs. 5 and 7) throughout both cores and the brief increases in the 1970s and 1980s may be due to shifts in nitrogen availability in Waterhen Lake (Schindler et al. 2008; Blais et al. 2012). The decline in Nostocales cyanobacteria (Figs. 5 and 6) may be due to increased nitrogen levels arising from upstream agricultural fertilizers via Lake Winnipegosis entering Waterhen Lake through the Little Waterhen River and the West Waterhen River (Statistics Canada 1961–2022; Patoine et al. 2006; Bunting et al. 2016; Galbraith et al. 2017; Soto et al. 2019). Although it is known that the fertilizer use in the Lake Winnipegosis catchment has increased since the 1960s, it is difficult to determine the level of nitrogen that has been transported into Waterhen Lake via Lake Winnipegosis over time (Statistics Canada 1961–2022; Galbraith et al. 2017). However, wetlands tend to be nitrogen-limited prior to agricultural runoff and tend to sequester nitrogen (Morris 1991; Nilsson et al. 2023). This means that inputs into Waterhen Lake are likely very low in nitrogen (Morris 1991; Nilsson et al. 2023). Atmospheric deposition of inorganic nitrogen ($NH_3$) arising from N-fertilizer (e.g., liquid

ammonium, urea) application may also be increasing the nitrogen availability in Waterhen Lake (Bergström and Jansson 2006; Cao et al. 2020). Atmospheric deposition of nitrogen is known to have caused increased eutrophication in nitrogen limited systems in the northern hemisphere throughout the 20$^{th}$ century (Bergström and Jansson 2006). In Waterhen Lake, increased nitrogen inputs from non-local sources (atmospheric) may be increasing phytoplankton growth but limiting Nostocales abundance since they are competitively dominant under low nitrogen conditions (Bergström and Jansson 2006; Grover et al. 2022). The increasing trends of cyanobacteria as echinenone in core 1 and colonial cyanobacteria (myxoxanthophyll) in both cores (Figs. 5 and 7) confirm that eutrophication is occurring in the lake likely due to increased nutrient availability (i.e., nitrogen) and internal phosphorous loading from the sediment during anoxic conditions as mentioned above (Halac et al. 2020; Tammeorg et al. 2020). Additionally, the water chemistry data obtained from the Centre for Earth Observational Science shows a mean TDN:TDP ratio of ~30 (Appendix A, Table 1), indicating that there is much more nitrogen available in the lake than phosphorous. This confirms that although nitrogen was likely limiting in the past, it is not the limiting nutrient now and nitrogen-fixing cyanobacteria have lost their competitive advantage (Blais et al. 2012; Grover et al. 2022). Although it is difficult to determine at this stage where the nitrogen is originating from, or if nitrogen inputs are indeed increasing, future analysis of sediment $\delta^{15}N$ isotope ratios will indicate if there is increased nitrogen deposition to the lake and there are changes in nitrogen fixation by the cyanobacteria communities ($\delta^{15}N$ declines during elevated periods of nitrogen fixation) (Patoine et al. 2006).

Since the pigments lutein (chlorophytes) and zeaxanthin (cyanobacteria) co-elute during the HPLC process, the pigments were interpreted together in the grouping of "bloom-forming taxa" (Cottingham et al. 2000; Leavitt and Hodgson 2001). Chlorophytes (green algae) and cyanobacteria are non-related groups, which makes this pigment difficult to interpret (Leavitt and Hodgson 2001). In core 1, bloom-forming taxa appears to follow the trends of Nostocales cyanobacteria pigments in group one, which indicates that Nostocales cyanobacteria are the main bloom-forming taxa during this period (Fig. 5). In group two, Nostocales cyanobacteria declines while bloom-forming taxa pigment concentrations stay relatively constant, indicating that green algae and colonial cyanobacteria are the major bloom-forming taxa during this period (Fig. 5). Additionally, at the end of group two (ca. 2020) the bloom-forming taxa declines along with the green algae and the colonial cyanobacteria, indicating that during this period bloom-forming taxa continues to be made up of green algae and colonial cyanobacteria (Fig. 5). In core 2, the bloom-forming taxa is likely contributed to the most by Nostocales cyanobacteria in the first group, with the large decline in concentration ca. 1950–1970 possibly from increased dissolved organic carbon in the lake, as mentioned previously (Fig. 7). In the second group, bloom-forming taxa remains elevated despite the decline in Nostocales cyanobacteria indicating that green algae and colonial cyanobacteria contributed majorly to algal blooms after the 1970s (Fig. 7).

Chlorophyll a: pheophytin a ratios demonstrate differing degradation trends for pigments in each core (Figs. 6 and 8). Initial rates of degradation are rapid, however core 1 has a higher ratio initially (Fig. 6), indicating that there is greater fresh material in recent sediments and higher amounts of sediment deposition (Fig. 8) (Leavitt 1993; Leavitt and

Hodgson 2001). In both cores, the ratio shows a general trend of being below one prior to the 2000s, indicating that in the majority of each core the fresh material has degraded by this time (Leavitt 1993; Leavitt and Hodgson 2001). In core 2, there are several fluctuations throughout the early to mid-1900s, indicating that degradation is still occurring within the core, or that there were environmental changes during those periods (e.g., decreases in light penetration in the water column) that altered the degradation process of the pigments (Fig. 8) (Leavitt 1993; Leavitt and Hodgson 2001). These trends in the chlorophyll a: pheophytin ratio are typically of a large shallow lake, so there is confidence that the changes in pigment concentration that are occurring throughout the cores are due to environmental shifts and not simply poor preservation (Reavie et al. 2017).

Although the majority of the pigment concentration data shows similar trends within each core and between the cores, there are conflicts in some groups. Total algal abundance pigments present in core 1 exhibit slightly different trends, as β-carotene exhibits a variable trend ca. 2000, while pheophytin a does not (Fig. 5). This trend is likely due to the inherent structure of the HPCL process, as the β-carotene pigment is a heavy molecule and is the last to be detected in an HPLC run at the final stage of the stationary phase (Leavitt and Hodgson 2001). Therefore, the counter indication between β-carotene and pheophytin a is likely due to a potentially lower or less stable amount of mobile phase (i.e., pigment extract) during the end of the analysis (Leavitt 1993; Leavitt and Hodgson 2001). Given the general consistency between pheophytin a and most other pigment trends within both cores we are confident that this pigment is a more accurate marker of overall production in the lake. Further, there are major differences between

cores in the concentrations of echinenone and diatoxanthin. In core 1, diatom pigment concentration (diatoxanthin) exhibits a declining trend, while in core 2 diatom pigment concentrations exhibit an increasing trend (Figs. 5 and 7). The differences in diatom pigment concentrations between cores may be due to the cores being extracted from different locations in the basin. Core 1 is from the more central, deeper basin, while core 2 is from the shallower slope of the basin (Table 1). Core 1 is more central to the basin, so trends observed in core 1 are likely more reflective of the overall lake environment.

*Diatoms*

Diatom assemblages from core 1 showed that there has been a shift towards higher abundances of planktonic diatom taxa through time, particularly from the beginning of the CONISS group ca. 1975 (Fig. 9). The ca. 1975 break in the diatom data corresponds with the significant changes in the pigment concentrations (ca. 1974 core 1, ca. 1978 core 2) (Figs. 5 and 7). There is another major CONISS group beginning ca. 2023, which separated only one diatom sample (i.e., 0.0-0.5 cm) from the rest (Fig. 9). This significant break could indicate a major change in the diatom community and overall lake environment in recent years, but this is difficult to say concretely with one sample.

Changes in diatom community composition in Waterhen Lake indicate that thermal stability has likely increased (Rühland et al. 2015). Waterhen Lake is a large lake, consequently under warmer air temperatures there may be minimal fluctuations in water temperature, and the lake may hold the heat late in the season extending periods of thermal stability (Galbraith et al. 2017; Li et al. 2026). Increased thermal stability in lakes is a common outcome of climate change (Rühland et al. 2013). Waterhen Lake likely began experiencing increased thermal stability ca. 1970–1980, when the mean annual

temperature in the Waterhen Lake region increased substantially (Appendix B, Fig. 1) (ECCC 2025b; Li et al. 2026). Under increased thermal stability, planktonic diatoms benefit (Rühland et al. 2015). Planktonic diatom species are typically less silicified, and many planktonic taxa have body plans (e.g., long and thin) conducive to remain suspended in the water column (Rühland et al. 2015). These long, thin planktonic diatoms include *Fragilaria tenera, Fragilaria nanana,* and *Astrionella* species, which are present in Waterhen Lake and have increased in more recent sediments (Figs. 9 and 10) (Tolotti et al. 2007; Rühland et al. 2013; Rühland et al. 2015). Staying suspended in the water column allows these diatom species to retain access to light while outcompeting other, more heavily silicified planktic species (e.g., *Aulocoseira* species.; Fig. 10) and benthic/tychoplanktonic species (e.g., *Pseudostaurosira brevistriata* and *Staurosirella pinnata*; Figs. 9 and 10) that require turbulence to remain suspended (Moos et al. 2005; Rühland et al. 2008; Michelutti et al. 2015; Liu et al. 2020; Sivarajah et al. 2022). Additionally, a switch from benthic to plankton diatom taxa may also indicate increased production in Waterhen Lake (Rühland et al. 2015; Liu et al. 2020). As mentioned above, there has been an increase in fertilizer application upstream of Waterhen Lake, which may be leading to increased nutrient availability in the lake through nutrients entering through inflows, or, through atmospheric deposition (Statistics Canada 1961–2022; Bergström and Jansson 2006). In many lakes there have been increases in plankton *Fragilaria* and *Asterionella* in association with increased nutrient availability (e.g., nitrogen) and warming from climate change (Rühland et al. 2015; Sivarajah et al. 2016; Griffiths et al. 2022). Elevated temperatures and potentially nutrient availability in Waterhen Lake ca. 1970 onwards parallel increased plankton *Fragilaria*, which has also increased since the 1970s (Fig. 9) (Statistics Canada 1961–2022; ECCC 2025b). Similar to thermal stability,

when nutrient availability and production is higher in the lake, there is higher algal biomass (e.g., positively buoyant cyanobacteria, planktonic diatoms) at the surface of the water which blocks light to algae, such as benthic diatoms, causing planktonic diatom taxa to become more abundant (Viner 1985; Rühland et al. 2013, 2015; Pick 2016; Liu et al. 2020). Additionally, ca. 1975 and throughout the fourth group (1975–2023) there were declines in small, generalist, benthic taxa such as *Pseudostaurosira brevistriata*, *Staurosirella pinnata*, and *Amphora pediculus* (Fig. 9), and the PCA results show that these species are highly associated with each other (Fig. 10) (Rzodkiewicz et al. 2026). These species prefer oligotrophic – mesotrophic conditions and require turbulence to thrive, so declines in these taxa could indicate that Waterhen Lake is increasing in trophic status throughout this period (Michelutii et al. 2015; Sivarajah et al. 2022; Rzodkiewicz et al. 2026).

Diatoxanthin concentrations were used to infer diatom concentration demonstrating that in addition to changes in diatom taxa in core 1, there have also been changes in diatom concentrations (Foets et al. 2020; Bjorndahl et al. 2022). As discussed earlier, core 1 exhibits a trend of decreasing diatom pigment concentrations (diatoxanthin) through time, while core 2 shows increasing diatom pigment concentrations through time (Figs. 5 and 7). This difference may be due to core 1 being taken from a deeper location (Table 1), where light penetration through the water column has decreased through time, causing the shift to increased planktonic diatom taxa (Figs. 9 and 10) and an overall lower concentration of diatoms (Fig. 5) (Liu et al. 2020; Hofmann et al. 2020). Whereas core 2 was taken from shallower location in the lake (Table 1) where higher light levels may have continuously reached the bottom through time, potentially supporting a robust

benthic diatom population through time (Hofmann et al. 2020). In the future, the analysis of core 2 diatom assemblages will provide greater insight into why this difference is occurring. In core 1, there were five significant groups in the CONISS test including three secondary CONISS groups beginning ca. 1892, 1900, and 1963 (Fig. 9). The diatom taxa sample size was much smaller than the pigment concentration sample size, which may have led to a larger number of significant groups in the diatom data than the pigment data. Analyzing diatom samples at additional depths may result in more consistent results with the pigments. Due to the smaller sample size, the diatom data is being used more supplementary to the findings of the pigment concentrations in this thesis.

*Food-web implications*

The food-web in Waterhen Lake appears to be controlled from the bottom up (Bhele et al. 2022). Walleye were stocked in Waterhen Lake starting in 2003; however, pigment concentrations show little change in composition and indicate little change in lake production during this period (Figs. 5 and 7) (Galbraith et al. 2017). This trend indicates that nutrients and climate change are likely having the largest effect on production in Waterhen Lake, and trophic cascades are likely controlled from the bottom up (Bhele et al. 2022). Changes that have occurred in the phytoplankton are likely impacting predatory fish, such as walleye and northern pike (Tunney et al. 2018; Bhele et al. 2022). The increase in total algal production beginning ca. 1970–1980 is likely providing more food to zooplankton, which in turn provides more food and increasing population sizes of prey fish species that predatory fish consume (Tunney et al. 2018; Bhele et al. 2022). Despite the potential increase in prey for walleye and northern pike, the increase in production is also likely to have negative impacts (Viner 1985; Moos et al. 2005; Rühland et al. 2008, 2013, 2015; Michelutti et al. 2015; Pick 2016; Terry et al. 2017; Nieman et al. 2018; Liu

et al. 2020; Sivarajah et al. 2022). As mentioned previously, increased production creates anoxia in the water causing fish kills (Terry et al. 2017). Anoxia may be killing walleye and northern pike directly and killing prey fish, decreasing the food supply for the predatory fish (Terry et al. 2017). Additionally, the shift to planktonic diatom taxa suggests that light penetration has likely decreased in the lake, potentially harming walleye hunting ability (Viner 1985; Moos et al. 2005; Rühland et al. 2008, 2013, 2015; Michelutti et al. 2015; Pick 2016; Nieman et al. 2018; Liu et al. 2020; Sivarajah et al. 2022). Future studies should examine zooplankton populations through time to gain more knowledge into changes in the Waterhen Lake food-web and how these changes are impacting the fishery.

**Conclusion**

In conclusion, pigment concentration and diatom relative abundance results indicate that long-term climate change beginning ca. 1970–1980 has likely caused increased phytoplankton production to occur in Waterhen Lake through increases in temperature (primarily increased mean annual and winter temperatures) and longer periods of thermal stability (Winter et al. 2011; Rühland et al. 2015; Ho et al. 2019; Liu et al. 2020; Griffiths et al. 2022; Li et al. 2022; ECCC 2025b; Rzodkiewicz et al. 2026). Additionally, possible increases in nutrient inputs have likely resulted in shifts in phytoplankton composition that favour non-nitrogen-fixing cyanobacteria (Schindler et al. 2008; Blais et al. 2012; Rühland et al. 2015; Liu et al. 2020). Together, these results suggest that increased biological production has degraded the water quality of Waterhen Lake through time and may impact fisheries health as further climate and nutrient cycling effects increase periods of anoxia (Barica and Mathias, 1979; McMahon et al., 1984; Stewart et al., 2016; Raabe et al., 2020). Further, this study highlights how large BPE lakes are affected by multiple

stressors and that local fishers and managers should be prepared to adapt to a changing lake ecosystem.

**Literature Cited**

Agriculture and Agri-Food Canada (AAFC). 2023. Annual Crop Inventory. Available from https://open.canada.ca/data/en/dataset/ba264 5d5- 4458- 414db196-6303a c06c1c9 [Accessed September 2025].

Appleby, P.G., and Oldfieldz, F. 1983. The assessment of 210Pb data from sites with varying sediment accumulation rates. Hydrobiologia, **103**: 29–35. doi:10.1007/BF00028424.

Appleby, P.G., Nolan, P.J., Gifford, D.W., Godfrey, M.J., Oldfield, F., Anderson, N.J., and Battarbee, R.W. 1986. 210Pb dating by low background gamma counting. Hydrobiologia, **143**: 21–27. doi:10.1007/BF00026640.

Aquino-Lopez, M.A., Blaauw, M., Christen, J.A., and Sanderson, N. 2018. Bayesian analysis of 210Pb dating. J. Agri. Biol. Environ. Stat. **23**: 317–333. doi: 10.1007/s13253-018-0328-7.

Barica, J., and Mathias, J.A. 1979. Oxygen depletion and winterkill risk in small prairie lakes under extended ice cover. J. Fish. Res. Bd. Can. **36**: 980–986. doi:10.1139/f79-136.

Bastviken, D., and Johnson, M.S. 2025. Future methane emissions from lakes and reservoirs. Nat. Water. **3**: 1397–1410. doi:10.1038/s44221-025-00532-6.

Battarbee, R.W., Jones, V.J., Flower, R.J., Cameron, N.G., Bennion, H., Carvalho, L., Juggins, S., Smol, J.P., Birks, H.J.B., Last, W.M., Bradley, R.S., and Alverson K. 2001. Diatoms. *In* Tracking environmental change using lake sediments: Terrestrial, algal, and siliceous indicators. *Edited by* Smol, J.P., Birks, H.J.B., Last,

W.M., Bradley, R.S., and Alverson, K. Springer, Netherlands, Dordrecht. pp. 155–202.

Bayley, S.E., Wong, A.S., and Thompson, J.E. 2013. Effects of agricultural encroachment and drought on wetlands and shallow lakes in the Boreal Transition Zone of Canada. Wetlands, **33**: 17–28. doi:10.1007/s13157-012-0349-x.

Benoit, G., and Rozan, T.F. 2001. $^{210}$Pb and $^{137}$Cs dating methods in lakes: A retrospective study. J. Paleolimnol. **25**: 455–465. doi:10.1023/A:1011179318352.

Bergström, A.-K., and Jansson, M. 2006. Atmospheric nitrogen deposition has caused nitrogen enrichment and eutrophication of lakes in the northern hemisphere. Glob. Chang. Biol. **12**: 635–643. doi:10.1111/j.1365-2486.2006.01129.x.

Beutel, M.W. 2003. Hypolimnetic anoxia and sediment oxygen demand in California drinking water reservoirs. Lake Reserv. Manag. **19**: 208–221. doi:10.1080/07438140309354086.

Beutel, M.W. 2006. Inhibition of ammonia release from anoxic profundal sediments in lakes using hypolimnetic oxygenation. Ecol. Eng. **28**: 271–279. doi:10.1016/j.ecoleng.2006.05.009.

Bhele, U., Öğlü, B., Feldmann, T., Bernotas, P., Agasild, H., Zingel, P., Nõges, P., Nõges, T., and Cremona, F. 2022. Modelling how bottom-up and top-down processes control the major functional groups of biota in a large temperate shallow lake. Inland Waters, **12**: 368–382. doi:10.1080/20442041.2022.2031813.

Binford, M. 1990. Calculation and uncertainty analysis of $^{210}$Pb dates for PIRLA project lake sediment cores. J. Paleolimnol. **3**: doi:10.1007/BF00219461.

Binford, M.W., Kahl, J.S., and Norton, S.A. 1993. Interpretation of $^{210}$Pb profiles and verification of the CRS dating model in PIRLA project lake sediment cores. J Paleolimnol. **9**: 275–296. doi:10.1007/BF00677218.

Bjorndahl, J.A., Gushulak, C.A.C., Mezzini, S., Simpson, G.L., Haig, H.A., Leavitt, P.R., and Finlay, K. 2022. Abrupt changes in the physical and biological structure of endorheic upland lakes due to 8-m lake-level variation during the 20th century. Limnol. Oceanogr. **67**: 1022–1039. doi:10.1002/lno.12054.

Blais, M., Tremblay, J.-É., Jungblut, A.D., Gagnon, J., Martin, J., Thaler, M., and Lovejoy, C. 2012. Nitrogen fixation and identification of potential diazotrophs in the Canadian Arctic. Global Biogeochem. Cy. **26**: GB3022. doi:10.1029/2011GB004096.

Boström, B., Andersen, J.M., Fleischer, S., and Jansson, M. 1988. Exchange of phosphorus across the sediment-water interface. Hydrobiologia, **170**: 229–244. doi:10.1007/BF00024907.

Brown, L.C., and Duguay, C.R. 2011. The fate of lake ice in the North American Arctic. Cryosphere, **5**: 869–892. doi:10.5194/tc-5-869-2011.

Bunting, L., Leavitt, P. R., Simpson, G. l., Wissel, B., Laird, K. R., Cumming, B. F., St. Amand, A., and Engstrom, D.R. 2016. Increased variability and sudden ecosystem state change in Lake Winnipeg, Canada, caused by 20th century agriculture. Limnol. Oceanogr. **61**: 2090–2107. doi:10.1002/lno.10355.

Burge, D.R.L., Edlund, M.B., and Frisch, D. 2018. Paleolimnology and resurrection ecology: The future of reconstructing the past. Evol. Appl. **11**: 42–59. doi:10.1111/eva.12556.

Cao, P., Lu, C., Zhang, J., and Khadilkar, A. 2020. Northwestward cropland expansion and growing urea-based fertilizer use enhanced $NH_3$ emission loss in the contiguous United States. Atmos. Chem. Phys. **20**: 11907–11922. doi:10.5194/acp-20-11907-2020.

Carpenter, S.R., Cole, J.J., Kitchell, J.F., and Pace, M.L. 1998. Impact of dissolved organic carbon, phosphorus, and grazing on phytoplankton biomass and production in experimental lakes. Limnol. Oceanogr. **43**: 73–80. doi:10.4319/lo.1998.43.1.0073.

Casselman, J., Colby, P., and Scott, I. 2024. Waterhen Lake walleye and northern pike gillnet commercial fishery. Interteck fisheries certification and Marine Stewardship Council. Available from https://www.gov.mb.ca/nrnd/fish-wildlife/pubs/fish_wildlife/fish/certreport2014.pdf [accessed September 2025].

Chapra, S. 2008. Surface water-quality monitoring. Waveland Press Inc, Long Grove, Illinois.

Cormier, J.M., Coffin, M.R.S., Pater, C.C., Knysh, K.M., Gilmour, R.F., Guyondet, T., Courtenay, S.C., and van den Heuvel, M.R. 2023. Internal nutrients dominate load and drive hypoxia in a eutrophic estuary. Environ. Monit. Assess. **195**: 1211. doi:10.1007/s10661-023-11621-y.

Cottingham, K.L., Rusak, J.A., and Leavitt, P.R. 2000. Increased ecosystem variability and reduced predictability following fertilisation: Evidence from palaeolimnology. Ecol. Lett. **3**: 340–348. doi:10.1046/j.1461-0248.2000.00158.x.

Dean, W.E. 1974. Determination of carbonate and organic matter in calcareous sediments and sedimentary rocks by loss on ignition; comparison with other methods. J.

Sediment. Res. **44**: 242–248. doi:10.1306/74D729D2-2B21-11D7-8648000102C1865D.

Dean, W.E. 1999. The carbon cycle and biogeochemical dynamics in lake sediments. J. Paleolimnol. **21**: 375–393. doi:10.1023/A:1008066118210.

Devlin, M., and Brodie, J. 2023. Nutrients and eutrophication. *In* Marine pollution – Monitoring, management and mitigation. *Edited by* Reichelt-Brushett, A. Springer Nature, Switzerland. pp. 75–100.

Dixit, S.S., Smol, J.P., Kingston, J.C., and Charles, D.F. 1992. Diatoms: powerful indicators of environmental change. Environ. Sci. Technol. **26**: 22–33. doi:10.1021/es00025a002.

Dixit, A.S., Hall, R.I., Leavitt, P.R., Quinlan, R., and Smol, J.P. 2000. Effects of sequential depositional basins on lake response to urban and agricultural pollution: a palaeoecological analysis of the Qu'Appelle Valley, Saskatchewan, Canada. Freshw. Biol. **43**: 319–337. doi:10.1046/j.1365-2427.2000.00516.x.

Donald, D.B., Parker, B.R., Davies, J.M., and Leavitt, P.R. 2015. Nutrient sequestration in the Lake Winnipeg watershed. J. Great Lakes Res. **41**: 630–642. doi:10.1016/j.jglr.2015.03.007.

Dunnington, D. W., Libera, N., Kurek, J., Spooner, I. S., and Gagnon, G. A. 2022. *tidypaleo*: Visualizing paleoenvironmental archives using *ggplot2*. J. Stat. Softw. **101**: 1-20. doi:10.18637/jss.v101.i07.

Eakins, J.D., and Morrison, R.T. 1978. A new procedure for the determination of lead-210 in lake and marine sediments. Int. J. Appl. Radiat. Isot. **29**: 531–536. doi:10.1016/0020-708X(78)90161-8.

Environment and Climate Change Canada (ECCC). 2010. Phosphorus in aquatic ecosystems: Chapter 2. Available from https://www.canada.ca/en/environment-climate-change/services/freshwater-quality-monitoring/publications/phosphorus-aquatic-ecosystems/chapter-2.html [Accessed March 2026].

Environment and Climate Change Canada (ECCC). 2025a. Adjusted and homogenized Canadian climate data; Precipitation. Available from https://www.canada.ca/en/environment-climate-change/services/climate-change/science-research-data/climate-trends-variability/adjusted-homogenized-canadian-data/precipitation-access.html [Accessed November 2025].

Environment and Climate Change Canada (ECCC). 2025b. Adjusted and homogenized Canadian climate data; Surface air temperature. Available from https://www.canada.ca/en/environment-climate-change/services/climate-change/science-research-data/climate-trends-variability/adjusted-homogenized-canadian-data/surface-air-temperature.html [Accessed November 2025].

Foets, J., Wetzel, C.E., Teuling, A.J., and Pfister, L. 2020. Temporal and spatial variability of terrestrial diatoms at the catchment scale: controls on productivity and comparison with other soil algae. PeerJ, **8**: e9198. doi:10.7717/peerj.9198.

Foley, B., Jones, I.D., Maberly, S.C., and Rippey, B. 2012. Long-term changes in oxygen depletion in a small temperate lake: effects of climate change and eutrophication. Freshw. Biol. **57**: 278–289. doi:10.1111/j.1365-2427.2011.02662.x.

Fork, M.L., Karlsson, J., and Sponseller, R.A. 2020. Dissolved organic matter regulates nutrient limitation and growth of benthic algae in northern lakes through interacting effects on nutrient and light availability. Limno. Oceanogr. Lett. **5**: 417–424. doi:10.1002/lol2.10166.

Friesen-Hughes, K., Casson, N.J., and Wilson, H.F. 2021. Nitrogen dynamics and nitrogen-to-phosphorus stoichiometry in cold region agricultural streams. J. Environ. Qual. **50**: 653–666. doi:10.1002/jeq2.20234.

Gaeta, J.W., Sass, G.G., and Carpenter, S.R. 2014. Drought-driven lake level decline: effects on coarse woody habitat and fishes. Can. J. Fish. Aquat. Sci. **71**: 315–325. doi:10.1139/cjfas-2013-0451.

Galbraith, W., Klein, G.M., and Kirbyson, G. 2017. Waterhen Lake summary report. Manitoba Sustainable Development, Province of Manitoba, Winnipeg, Manitoba.

Glew, J. R. 1989. A new trigger mechanism for sediment samplers. J. Paleolimnol. **2**: 241–243. doi:10.1007/BF00195474.

Google Earth 7.3. 2025. Waterhen Lake, Manitoba. Available from https://earth.google.com/web/ [accessed 23 August 2025].

Gorsky, A.L., Dugan, H.A., Wilkinson, G.M., and Stanley, E.H. 2024. Under-ice oxygen depletion and greenhouse gas supersaturation in north temperate urban ponds. J. Geophys. Res. BioGeosci. **129**: e2024JG008120. doi:10.1029/2024JG008120.

Griffiths, R.W., Schloesser, D.W., Leach, J.H., and Kovalak, W.P. 1991. Distribution and dispersal of the zebra mussel (*Dreissena polymorpha*) in the Great Lakes Region. Can. J. Fish. Aquat. Sci. **48**: 1381–1388. doi:10.1139/f91-165.

Griffiths, K., Jeziorski, A., Antoniades, D., Beaulieu, M., Smol, J.P., and Gregory-Eaves, I. 2022. Pervasive changes in algal indicators since pre-industrial times: A paleolimnological study of changes in primary production and diatom assemblages from ~200 Canadian lakes. Sci. Total Enviro. **838**: 155938–155938. doi:10.1016/j.scitotenv.2022.155938.

Grimm, E.C. 1987. CONISS: a FORTRAN 77 program for stratigraphically constrained cluster analysis by the method of incremental sum of squares. Comput. Geosci. **13**: 13–35. doi:10.1016/0098-3004(87)90022-7.

Grover, J.P., Scott, J.T., Roelke, D.L., and Brooks, B.W. 2022. Competitive superiority of N-fixing cyanobacteria when fixed N is scarce: Reconsiderations based on a model with heterocyst differentiation. Ecol. Model. **466**: 109904. doi:10.1016/j.ecolmodel.2022.109904.

Guildford, S.J., and Hecky, R.E. 2000. Total nitrogen, total phosphorus, and nutrient limitation in lakes and oceans: Is there a common relationship? Limno. Oceanogr. **45**: 1213–1223. doi:10.4319/lo.2000.45.6.1213.

Gushulak, C.A.C., Mezzini, S., Moir, K.E., Simpson, G.L., Bunting, L., Wissel, B., Engstrom D.R., Laird K.R., St. Amand A., Cumming, B.F., and Leavitt, P.R. 2024. Impacts of a century of land-use change on the eutrophication of large, shallow, prairie Lake Manitoba in relation to adjacent Lake Winnipeg (Manitoba, Canada). Freshw. Biol. **69**: 47–63. doi:10.1111/fwb.14192.

Halac, S., Mengo, L., Guerra, L., Lami, A., Musazzi, S., Loizeau, J.L., Ariztegui, D., and Piovano, E.L. 2020. Paleolimnological reconstruction of the centennial eutrophication processes in a sub-tropical South American reservoir. J. South Am. Earth Sci. **103**: 102707. doi:10.1016/j.jsames.2020.102707.

Hall, R.I., Leavitt, P.R., Quinlan, R., Dixit, A.S., and Smol, J.P. 1999. Effects of agriculture, urbanization, and climate on water quality in the northern Great Plains. Limnol. Oceanogr. **44**: 739–756. doi:10.4319/lo.1999.44.3_part_2.0739.

Hall, L.J., Emilson, E.J.S., Edwards, B., and Watmough, S.A. 2021. Patterns and trends in lake concentrations of dissolved organic carbon in a landscape recovering from environmental degradation and widespread acidification. Sci. Total Environ. **765**: 142679. doi:10.1016/j.scitotenv.2020.142679.

Hansen, G.J.A., Winslow, L.A., Read, J.S., Treml, M., Schmalz, P.J., and Carpenter, S.R. 2019. Water clarity and temperature effects on walleye safe harvest: an empirical test of the safe operating space concept. Ecosphere, **10**: e02737. doi:10.1002/ecs2.2737.

Heinsalu, A., Luup, H., Alliksaar, T., Nõges, P., and Nõges, T. 2008. Water level changes in a large shallow lake as reflected by the plankton:periphyton-ratio of sedimentary diatoms. Hydrobiologia, **599**: 23–30. doi:10.1007/s10750-007-9206-y.

Heiri, O., Lotter, A.F., and Lemcke, G. 2001. Loss on ignition as a method for estimating organic and carbonate content in sediments: reproducibility and comparability of results. J. Paleolimnol. **25**: 101–110. doi:10.1023/A:1008119611481.

Hilt, S., Köhler, J., Adrian, R., Monaghan, M.T., and Sayer, C.D. 2013. Clear, crashing, turbid and back – long-term changes in macrophyte assemblages in a shallow lake. Freshw. Biol. **58**: 2027–2036. doi:10.1111/fwb.12188.

Ho, J.C., Michalak, A.M., and Pahlevan, N. 2019. Widespread global increase in intense lake phytoplankton blooms since the 1980s. Nature, **574**: 667–670. doi:10.1038/s41586-019-1648-7.

Hofmann, A.M., Geist, J., Nowotny, L., and Raeder, U. 2020. Depth-distribution of lake benthic diatom assemblages in relation to light availability and substrate: implications for paleolimnological studies. J. Paleolimnol. **64**: 315–334. doi:10.1007/s10933-020-00139-9.

Horppila, J., Keskinen, S., Nurmesniemi, M., Nurminen, L., Pippingsköld, E., Rajala, S., Sainio, K., and Estlander, S. 2023. Factors behind the threshold-like changes in lake ecosystems along a water colour gradient: The effects of dissolved organic carbon and iron on euphotic depth, mixing depth and phytoplankton biomass. Freshw. Biol. **68**: 1031–1040. doi:10.1111/fwb.14083.

Howarth, R., Chan, F., Conley, D.J., Garnier, J., Doney, S.C., Marino, R., and Billen, G. 2011. Coupled biogeochemical cycles: eutrophication and hypoxia in temperate estuaries and coastal marine ecosystems. Front. Ecol. Environ. **9**: 18–26. doi:10.1890/100008.

Hu, K., Mushet, D.M., and Sweetman, J.N. 2023. Multiproxy paleolimnological records provide evidence for a shift to a new ecosystem state in the Northern Great Plains, USA. Limnol. Oceanogr. **68**: S54–S70. doi:10.1002/lno.12218.

Ireson, A.M., Barr, A.G., Johnstone, J.F., Mamet, S.D., Van der Kamp, G., Whitfield, C.J., Michel N.L., North, R.L., Westbrook, C.J., DeBeer, C., Chun, K.P., Nazemi, A., and Sagin, J. 2015. The changing water cycle: the Boreal Plains ecozone of Western Canada. WIREs Water, **2**: 505–521. doi:10.1002/wat2.1098.

Jolliffe, I.T., and Cadima, J. 2016. Principal component analysis: a review and recent developments. Philos. Trans. A. Math. Phys. Eng. Sci. **374**: 20150202. doi:10.1098/rsta.2015.0202.

Juggins, S. 2024. rioja: Analysis of quaternary science data. doi: 10.32614/CRAN.package.rioja.

Keller, W. 2007. Implications of climate warming for Boreal Shield lakes: a review and synthesis. Environ. Rev. **15**: 99–112. doi:10.1139/A07-002.

Krammer, K., and Lange-Bertalot, H. 1986. *Bacillariophyceae*. 1. Teil: *Naviculaceae*. *In* Süßwasserflora von Mitteleuropa. *Edited by* H. Ettl, G. Gärtner, J. Gerloff, H. Heynig, D. Mollenhauer. Gustav Fischer Verlag. Vol. 2/1, pp. 1- 876.

Krammer, K., and Lange-Bertalot, H. 1988. *Bacillariophyceae*. 2. Teil: *Bacillariaceae, Epithemiaceae, Surirellaceae*. *In* Süßwasserflora von Mitteleuropa. *Edited by* H. Ettl, G. Gärtner, J. Gerloff, H. Heynig, D. Mollenhauer. Gustav Fischer Verlag. Vol. 2/2, pp. 1- 596.

Krammer, K., and Lange-Bertalot, H. 1991a. *Bacillariophyceae*. 3. Teil: *Centrales, Fragilariaceae, Eunotiaceae*. *In* Süßwasserflora von Mitteleuropa. *Edited by* H. Ettl, G. Gärtner, J. Gerloff, H. Heynig, D. Mollenhauer. Gustav Fischer Verlag. Vol. 2/3, pp. 1 - 576.

Krammer, K., and Lange-Bertalot, H. 1991b. *Bacillariophyceae*. 4. Teil: *Achnanthaceae*. *In* Süßwasserflora von Mitteleuropa. *Edited by* H. Ettl, G. Gärtner, J. Gerloff, H. Heynig, D. Mollenhauer. Gustav Fischer Verlag. Vol. 2/4, pp. 1 - 437.

Laird, K.R., and Cumming, B.F. 2008. Reconstruction of Holocene lake level from diatoms, chrysophytes and organic matter in a drainage lake from the Experimental Lakes Area (northwestern Ontario, Canada). Quat. Res. **69**: 292–305. doi:10.1016/j.yqres.2007.11.003.

Laird, K.R., Fritz, S.C., Grimm, E.C., and Mueller, P.G. 1996. Century scale paleoclimatic reconstruction from Moon Lake, a closed-basin lake in the northern Great Plains. Limnol. Oceanogr. **41**: 890–902. doi:10.4319/lo.1996.41.5.0890.

Leavitt, P.R. 1993. A review of factors that regulate carotenoid and chlorophyll deposition and fossil pigment abundance. J. Paleolimnol. **9**: 109–127. doi:10.1007/BF00677513.

Leavitt, P.R., and Hodgson, D.A. 2001. Sedimentary Pigments. *In* Tracking Environmental Change Using Lake Sediments: Terrestrial, Algal, and Siliceous Indicators. *Edited by* J.P. Smol, H.J.B. Birks, W.M. Last, R.S. Bradley, K. Alverson. Springer, Netherlands, Dordrecht. pp. 295–325.

Leavitt, P.R., Carpenter, S.R., and Kitchell, J.F. 1989. Whole-lake experiments: The annual record of fossil pigments and zooplankton. Limnol. Oceanogr. **34**: 700–717. doi:10.4319/lo.1989.34.4.0700.

Legendre, P., and Borcard, D. 2018. Box–Cox-chord transformations for community composition data prior to beta diversity analysis. Ecography, **41**: 1820–1824. doi:10.1111/ecog.03498.

Li, R., Kang, W., Chen, G., Chen, L., Zhao, S., Chen, X., and Zhang, T. 2026. Thermal stability overrides epilimnetic nutrient availability in diatom seasonality in a deep lake of subtropical China. J. Gt. Lakes Res. **52**: 102734. doi:10.1016/j.jglr.2025.102734.

Li, X., Peng, S., Xi, Y., Woolway, R.I., and Liu, G. 2022. Earlier ice loss accelerates lake warming in the Northern Hemisphere. Nat. Commun. **13**: 5156. doi:10.1038/s41467-022-32830-y.

Li, X., Hang, X., Zhu, S., Sun, L., and Li, Y. 2025. Response of cyanobacterial blooms to climate warming: evidence from satellite observations and long-term trends in Lake Taihu in China. Sci. Rep. **15**: 38820. doi:10.1038/s41598-025-22633-8.

Liu, B., Chen, S., Liu, H., and Guan, Y. 2020. Changes in the ratio of benthic to planktonic diatoms to eutrophication status of Muskegon Lake through time: Implications for a valuable indicator on water quality. Ecol. Indic. **114**: 106284. doi:10.1016/j.ecolind.2020.106284.

Maechler, M., Rousseeuw, P., Struyf, A., Hubert, M., and Hornik, K. 2025. *cluster*: Cluster analysis basics and extensions. doi: 10.32614/CRAN.package.cluster.

Malley, D.F., and Mills, K.H. 1992. Whole-lake experimentation as a tool to assess ecosystem health, response to stress and recovery: the Experimental Lakes Area experience. J. Aquat. Ecosyst. Stress Recov. **1**: 159–174. doi:10.1007/BF00044713.

Marine Stewardship Council (MSC). 2014. Marine Stewardship Council (MSC) fishery certificate. Intertek fisheries certification. Available from https://www.gov.mb.ca/nrnd/fish-wildlife/pubs/fish_wildlife/fish/msccert2014.pdf [accessed September 2025].

Marty, C., Duchesne, L., Couture, S., Gagnon, C., and Houle, D. 2021. Effects of climate and atmospheric deposition on a boreal lake chemistry: A synthesis of 36 years of monitoring data. Sci. Total Environ. **758**: 143639. doi:10.1016/j.scitotenv.2020.143639.

McDonald, K.E., and Lehman, J.T. 2013. Dynamics of *Aphanizomenon* and *Microcystis* (cyanobacteria) during experimental manipulation of an urban impoundment. Lake Reserv. Manage. **29**: 103–115. doi:10.1080/10402381.2013.800172.

McGowan, S., Leavitt, P.R., Hall, R.I., Anderson, N.J., Jeppesen, E., and Odgaard, B.V. 2005. Controls of algal abundance and community composition during Ecosystem State Change. Ecology, **86**: 2200–2211. doi:10.1890/04-1029.

McMahon, T.E., Terrell, J.W., and Nelson, P.C. 1984. Habitat Suitability Information: Walleye. Fish and Wildlife Service.

Meingast, K.M., Kane, E.S., Coble, A.A., Marcarelli, A.M., and Toczydlowski, D. 2020. Climate, snowmelt dynamics and atmospheric deposition interact to control dissolved organic carbon export from a northern forest stream over 26 years. Environ. Res. Lett. **15**: 104034. doi:10.1088/1748-9326/ab9c4e.

Michelutti, N., Cooke, C.A., Hobbs, W.O., and Smol, J.P. 2015. Climate-driven changes in lakes from the Peruvian Andes. J. Paleolimnol. **54**: 153–160. doi:10.1007/s10933-015-9843-5.

Moos, M., Laird, K.R., and Cumming, B.F. 2005. Diatom assemblages and water depth in Lake 239 (Experimental Lakes Area, Ontario): implications for paleoclimatic studies. J. Paleolimnol. **34**: 217–227. doi:10.1007/s10933-005-2382-8.

Morales-Marín, L.A., Wheater, H.S., and Lindenschmidt, K.E. 2017. Assessment of nutrient loadings of a large multipurpose prairie reservoir. J. Hydrol. **550**: 166–185. doi:10.1016/j.jhydrol.2017.04.043.

Morris, J.T. 1991. Effects of nitrogen loading on wetland ecosystems with particular reference to atmospheric deposition. Annu. Rev. Ecol. Syst. **22**: 257–279. doi:10.1146/annurev.es.22.110191.001353.

Nanayakkara, L. 2018. Prairie lakes: Model systems for integrating ecology and human dimensions for better management. Limnol. Oceanogr. Bull. **27**: 110–113. doi:10.1002/lob.10274.

Naselli-Flores, L., and Padisák, J. 2023. Ecosystem services provided by marine and freshwater phytoplankton. Hydrobiologia, **850**: 2691–2706. doi:10.1007/s10750-022-04795-y.

Nieman, C.L., Oppliger, A.L., McElwain, C.C., and Gray, S.M. 2018. Visual detection thresholds in two trophically distinct fishes are compromised in algal compared to sedimentary turbidity. Conserva. Physiol. **6**: coy044. doi:10.1093/conphys/coy044.

Nilsson, J.E., Weisner, S.E.B., and Liess, A. 2023. Wetland nitrogen removal from agricultural runoff in a changing climate. Sci. Total Environ. **892**: 164336. doi:10.1016/j.scitotenv.2023.164336.

Null, S.E., Mouzon, N.R., and Elmore, L.R. 2017. Dissolved oxygen, stream temperature, and fish habitat response to environmental water purchases. J. Environ. Manage. **197**: 559–570. doi:10.1016/j.jenvman.2017.04.016.

Nürnberg, G.K., and LaZerte, B.D. 2016. More than 20 years of estimated internal phosphorus loading in polymictic, eutrophic Lake Winnipeg, Manitoba. J. Great Lakes Res. **42**: 18–27. doi:10.1016/j.jglr.2015.11.003.

Pace, M.L., Cole, J.J., Carpenter, S.R., Kitchell, J.F., Hodgson, J.R., Van de Bogert, M.C., Bade, D.L., Kritzberg, E.S., and Bastviken, D. 2004. Whole-lake carbon-13 additions reveal terrestrial support of aquatic food webs. Nature, **427**: 240–243. doi:10.1038/nature02227.

Patoine, A., Graham, M.D., and Leavitt, P.R. 2006. Spatial variation of nitrogen fixation in lakes of the northern Great Plains. Limnol. Oceanogr. **51**: 1665–1677. doi:10.4319/lo.2006.51.4.1665.

Pick, F.R. 2016. Blooming algae: a Canadian perspective on the rise of toxic cyanobacteria. Can. J. Fish. Aquat. Sci. **73**: 1149–1158. doi:10.1139/cjfas-2015-0470.

Pienitz, R., Roberge, K., and Vincent, W.F. 2006. Three hundred years of human-induced change in an urban lake: paleolimnological analysis of Lac Saint-Augustin, Québec City, Canada. Can. J. Bot. **84**: 303–320. Doi:10.1139/B05-152.

Portielje, R., and Van der Molen, D.T. 1999. Relationships between eutrophication variables: from nutrient loading to transparency. Hydrobiologia, **408**: 375–387. doi:10.1023/A:1017090931476.

Province of Manitoba. 2024. Manitoba Geological Survey 2024: Bedrock Geology of Manitoba. Manitoba Economic Development, Investment, Trade and Natural Resources, Manitoba Geological Surveys.

Qin, B., Gao, G., Zhu, G., Zhang, Y., Song, Y., Tang, X., Hai, X., and Deng, J. 2013. Lake eutrophication and its ecosystem response. Chin. Sci. Bull. **58**: 961–970. doi:10.1007/s11434-012-5560-x.

Raabe, J.K., Van De Hey, J.A., Zentner, D.L., Cross, T.K., and Sass, G.G. 2020. Walleye inland lake habitat: considerations for successful natural recruitment and stocking in North Central North America. Lake Reserv. Manag. **36**: 335–359. doi:10.1080/10402381.2019.1697771.

R Core Team. 2025. R: A Language and Environment for Statistical Computing. R Foundation for Statistical Computing, Vienna, Austria. https://www.R-project.org/.

Reavie, E.D., Heathcote, A.J., and Shaw Chraïbi, V.L. 2014. Laurentian Great Lakes phytoplankton and their water quality characteristics, including a diatom-based model for paleoreconstruction of phosphorus. PLoS One, **9**: e104705. doi:10.1371/journal.pone.0104705.

Reavie, E.D., Edlund, M.B., Andresen, N.A., Engstrom, D.R., Leavitt, P.R., Schottler, S., and Cai, M. 2017. Paleolimnology of the Lake of the Woods southern basin: continued water quality degradation despite lower nutrient influx. Lake Reserv. Manag. **33**: 369–385. doi:10.1080/10402381.2017.1312648.

Reinl, K.L., Brookes, J.D., Carey, C.C., Harris, T.D., Ibelings, B.W., Morales-Williams, A.M., De Senerpont Domis, L.N., Atkins, K.S., Isles, P.D.F., Mesman, J.P., North,

R.L., Rudstam, L.G., Stelzer, J.A.A., Venkiteswaran, J.J., Yokota, K., and Zhan, Q. 2021. Cyanobacterial blooms in oligotrophic lakes: Shifting the high-nutrient paradigm. Freshw. Biol. **66**: 1846–1859. doi:10.1111/fwb.13791.

Robbins, J. A., 1978. Geochemical and geophysical applications of radioactive lead. *In* Biogeochemistry of Lead in the Environment. *Edited by* Nriagu, J. O. Elsevier Scientific, Amsterdam. pp. 285–393.

Robbins, J.A., Edgington, D.N., and Kemp, A.L.W. 1978. Comparative $^{210}$Pb, $^{137}$Cs, and Pollen Geochronologies of Sediments from Lakes Ontario and Erie. Quat. Res. **10**: 256–278. doi:10.1016/0033-5894(78)90105-9.

Rühland, K., Paterson, A.M., and Smol, J.P. 2008. Hemispheric-scale patterns of climate-related shifts in planktonic diatoms from North American and European lakes. Glob. Change Biol. **14**: 2740–2754. doi:10.1111/j.1365-2486.2008.01670.x.

Rühland, K.M., Paterson, A.M., Keller, W., Michelutti, N., and Smol, J.P. 2013. Global warming triggers the loss of a key Arctic refugium. Proc. Biol. Sci. **280**: 20131887. doi:10.1098/rspb.2013.1887.

Rühland, K.M., Paterson, A.M., and Smol, J.P. 2015. Lake diatom responses to warming: reviewing the evidence. J. Paleolimnol. **54**: 1–35. doi:10.1007/s10933-015-9837-3.

Rzodkiewicz, M., Zawiska, I., and Sobczak, M. 2026. Diatoms as indicators of eutrophication: Relationship with transparency, total phosphorus and chlorophyll-*a* concentration in Central European lakes. Glob. Ecol. Conserv. **65**: e04025. doi:10.1016/j.gecco.2025.e04025.

Sanger, J.E., and Gorham, E. 1970. The diversity of pigments in lake sediments and its ecological significance. Limnol. Oceanogr. **15**: 59–69. doi:10.4319/lo.1970.15.1.0059.

Schindler, D.W. 2009. Lakes as sentinels and integrators for the effects of climate change on watersheds, airsheds, and landscapes. Limnol. Oceanogr. **54**: 2349–2358. doi:10.4319/lo.2009.54.6_part_2.2349.

Schindler, D.W., Hecky, R.E., Findlay, D.L., Stainton, M.P., Parker, B.R., Paterson, M.J., Beaty, K.G., Lyng, M., and Kasian, S.E.M. 2008. Eutrophication of lakes cannot be controlled by reducing nitrogen input: Results of a 37-year whole-ecosystem experiment. Proc. Natl. Acad. Sci. **105**: 11254–11258. doi:10.1073/pnas.0805108105.

Schwefel, R., MacIntyre, S., Cortés, A., and Sadro, S. 2023. Oxygen depletion and sediment respiration in ice-covered arctic lakes. Limnol. Oceanogr. **68**: 1470–1489. doi:10.1002/lno.12357.

Sievert, C. 2020. Interactive web-based data visualization with R, *plotly*, and *shiny*. doi:10.32614/CRAN.package.plotly.

Sivarajah, B., Rühland, K.M., Labaj, A.L., Paterson, A.M., and Smol, J.P. 2016. Why is the relative abundance of *Asterionella formosa* increasing in a Boreal Shield lake as nutrient levels decline? J. Paleolimnol. **55**: 357–367. doi:10.1007/s10933-016-9886-2.

Sivarajah, B., Korosi, J.B., Thienpont, J.R., Kimpe, L.E., Blais, J.M., and Smol, J.P. 2022. Algal responses to metal(loid) pollution, urbanization, and climatic changes in

subarctic lakes around Yellowknife, Canada. Arct. Sci. **8**: 1340–1355. doi:10.1139/as-2021-0052.

Smol, J.P. 2010. The power of the past: using sediments to track the effects of multiple stressors on lake ecosystems. Freshw. Biol. **55**: 43–59. doi:10.1111/j.1365-2427.2009.02373.x.

Søndergaard, M., Bjerring, R., and Jeppesen, E. 2013. Persistent internal phosphorus loading during summer in shallow eutrophic lakes. Hydrobiologia, **710**: 95–107. doi:10.1007/s10750-012-1091-3.

Soto, D.X., Koehler, G., Wassenaar, L.I., and Hobson, K.A. 2019. Spatio-temporal variation of nitrate sources to Lake Winnipeg using N and O isotope ($\delta^{15}$N, $\delta^{18}$O) analyses. Sci. Total Environ. **647**: 486–493. doi:10.1016/j.scitotenv.2018.07.346.

Spaulding, S. A., Potapova, M. G., Bishop, I. W., Lee, S. S., Gasperak, T. S., Jovanoska, E., Furey, P. C., and Edlund, M. B. 2021. *Diatoms.org*: supporting taxonomists, connecting communities. Diatom Res. **36**: 291–304. https://doi.org/10.1080/0269249X.2021.2006790.

Statistics Canada. 1961-2021. Census of Agriculture. Available from https://www.statcan.gc.ca/en/census-agriculture [Accessed December 2025].

Stewart, E.M., Coleman, K.A., Korosi, J.B., Thienpont, J.R., Palmer, M.J., Blais, J.M., and Smol, J.P. 2016. Assessing environmental stressors on a commercial walleye fishery from a large northern ecosystem (Tathlina Lake) using water chemistry and paleolimnology. J. Great Lakes Res. **42**: 217–222. doi: 10.1016/j.jglr.2015.04.010.

Tammeorg, O., Nürnberg, G., Niemistö, J., Haldna, M., and Horppila, J. 2020. Internal phosphorus loading due to sediment anoxia in shallow areas: implications for lake aeration treatments. Aquat. Sci. **82**: 54. doi:10.1007/s00027-020-00724-0.

Tanentzap, A.J., Morabito, G., Volta, P., Rogora, M., Yan, N.D., and Manca, M. 2020. Climate warming restructures an aquatic food web over 28 years. Glob. Chang. Biol. **26**: 6852–6866. doi:10.1111/gcb.15347.

Tang, Y., Horikoshi, M., and Li, W. 2016. *ggfortify*: Unified interface to visualize statistic al result of popular R packages. R. J. **8**: 478-489. doi:10.32614/RJ-2016-00.

Terry, J.A., Sadeghian, A., and Lindenschmidt, K.-E. 2017. Modelling dissolved oxygen/s ediment oxygen demand under ice in a shallow eutrophic prairie reservoir. Water , **9**: 131. doi:10.3390/w9020131.

Thomas, M.K., and Litchman, E. 2016. Effects of temperature and nitrogen availability on the growth of invasive and native cyanobacteria. Hydrobiologia, **763**: 357–369. doi:10.1007/s10750-015-2390-2.

Tolotti, M., Corradini, F., Boscaini, A., and Calliari, D. 2007. Weather-driven ecology of planktonic diatoms in Lake Tovel (Trentino, Italy). Hydrobiologia, **578**: 147–156. doi:10.1007/s10750-006-0441-4.

Tunney, T.D., McCann, K.S., Jarvis, L., Lester, N.P., and Shuter, B.J. 2018. Blinded by the light? Nearshore energy pathway coupling and relative predator biomass increase with reduced water transparency across lakes. Oecologia, **186**: 1031–1041. doi:10.1007/s00442-017-4049-3.

Vadeboncoeur, Y., Jeppesen, E., M Jake Vander Zanden, Schierup, H.-H., Christoffersen, K., and Lodge, D.M. 2003. From Greenland to green lakes: Cultural

eutrophication and the loss of benthic pathways in lakes. Limnol. Oceanogra. **48**: 1408–1418. doi:10.4319/lo.2003.48.4.1408.

Viner, A.B. 1985. Thermal stability and phytoplankton distribution. Hydrobiologia, **125**: 47–69. doi:10.1007/BF00045925.

Waiser, M.J., and Robarts, R.D. 1997. Impacts of a herbicide and fertilizers on the microbial community of a saline prairie lake. Can. J. Fish. Aquat. Sci. **54**: 320–329. doi:10.1139/f96-280.

Watson, V.T., and Medeiros, A.S. 2021. The value of paleolimnology in reconstructing and managing ecosystem vulnerability: a systematic map. Facets, **6**: 517–536. doi:10.1139/facets-2020-0067.

Weber, S.J., Mishra, D.R., Wilde, S.B., and Kramer, E. 2020. Risks for cyanobacterial harmful algal blooms due to land management and climate interactions. Sci. Total Environ. **703**: 134608. doi:10.1016/j.scitotenv.2019.134608.

Webster, B.C., Smoak, J.M., Vachula, R.S., Waters, M.N., and Golladay, S.W. 2025. A comparison of dating models for reservoir sediment records using mass accumulation, radioisotopes, and Bayesian statistics. J. Paleolimnol. **74**: 1. doi:10.1007/s10933-025-00381-z.

Welch, E.B., Cooke, G.D., Jones, J.R., and Gendusa, T.C. 2011. DO–Temperature habitat loss due to eutrophication in Tenkiller Reservoir, Oklahoma, USA. Lake Reserv. Manag. **27**: 271–285. doi:10.1080/07438141.2011.607553.

Wetzel, R.G. 2001. Limnology: Lake and river ecosystems. 3rd ed. Academic Press, San Diego.

Wickham, H. 2016. *ggplot2*: Create elegant graphics for data visualization using the grammar of graphics. doi: 10.32614/CRAN.package.ggplot2.

Wickham, H., Vaughan, D., and Girlich, M. 2024. *tidyr*: Tidy messy data. doi:10.32614/CRAN.package.tidyr.

Wickham, H., François, R., Henry, L., Müller, K., and Vaughan, D. 2023. *dplyr*: A gram mar of data manipulation. doi:10.32614/CRAN.package.dplyr.

Wilke, C. 2025. *cowplot*: Streamlined plot theme and plot annotations for '*ggplot2*'. doi:10 .32614/CRAN.package.cowplot.

Winter, J.G., DeSellas, A.M., Fletcher, R., Heintsch, L., Morley, A., Nakamoto, L., and Utsumi, K. 2011. Algal blooms in Ontario, Canada: Increases in reports since 1994. Lake Reserv. Manag. **27**: 107–114. doi:10.1080/07438141.2011.557765.

Woolway, R.I., Sharma, S., Weyhenmeyer, G.A., Debolskiy, A., Golub, M., Mercado-Bettín, D., Perroud, M., Stepanenko, V., Tan, Z., Grant, L., Ladwig, R., Mesman, J., Moore, T.N., Shatwell, T., Vanderkelen, I., Austin, J.A., DeGasperi, C.L., Dokulil, M., La Fuente, S., Mackay, E.B., Schladow, S.G., Watanabe, S., Marcé, R., Pierson, D.C., Thiery, W., and Jennings, E. 2021. Phenological shifts in lake stratification under climate change. Nat. Commun. **12**: 2318. doi:10.1038/s41467-021-22657-4.

Woszczyk, M., Majewski, M., Schubert, C.J., and van Geldern, R. 2025. Trace gas ($CH_4$, $N_2O$, $H_2S$) distribution in the water column of inland lakes in Poland. Sci. Data. **13**: 58. doi:10.1038/s41597-025-06357-y.

Yang, B., Wells, M.G., Li, J., and Young, J. 2020. Mixing, stratification, and plankton under lake-ice during winter in a large lake: Implications for spring dissolved oxygen levels. Limnol. Oceanogr. **65**: 2713–2729. doi:10.1002/lno.11543.

Zaborska, A., Carroll, J., Papucci, C., and Pempkowiak, J. 2007. Intercomparison of alpha and gamma spectrometry techniques used in 210Pb geochronology. J. Environ. Radioact. **93**: 38–50. doi:10.1016/j.jenvrad.2006.11.007.

Zhang, F., Shi, X., Zhao, S., Hao, R., Sun, B., Song, S., and Li, G. 2024. Hypoxia cycle in shallow lakes during winter (ice-covered to melting period): Stable and decay, hypoxia, and recovery phases. Sci. Total Environ. **954**: 176625. doi:10.1016/j.scitotenv.2024.176625.

Zhao, L., Zhu, R., Zhou, Q., Jeppesen, E., and Yang, K. 2023. Trophic status and lake depth play important roles in determining the nutrient-chlorophyll *a* relationship: Evidence from thousands of lakes globally. Water Res. **242**: 120182. doi:10.1016/j.watres.2023.120182.

**Figures**

Fig. 1. Map of the Boreal Plains ecozone from Ireson et al. 2015, which is the ecozone Waterhen Lake is located in. Map is available from https://doi-org.uml.idm.oclc.org/10.1002/wat2.1098, Figure 1.

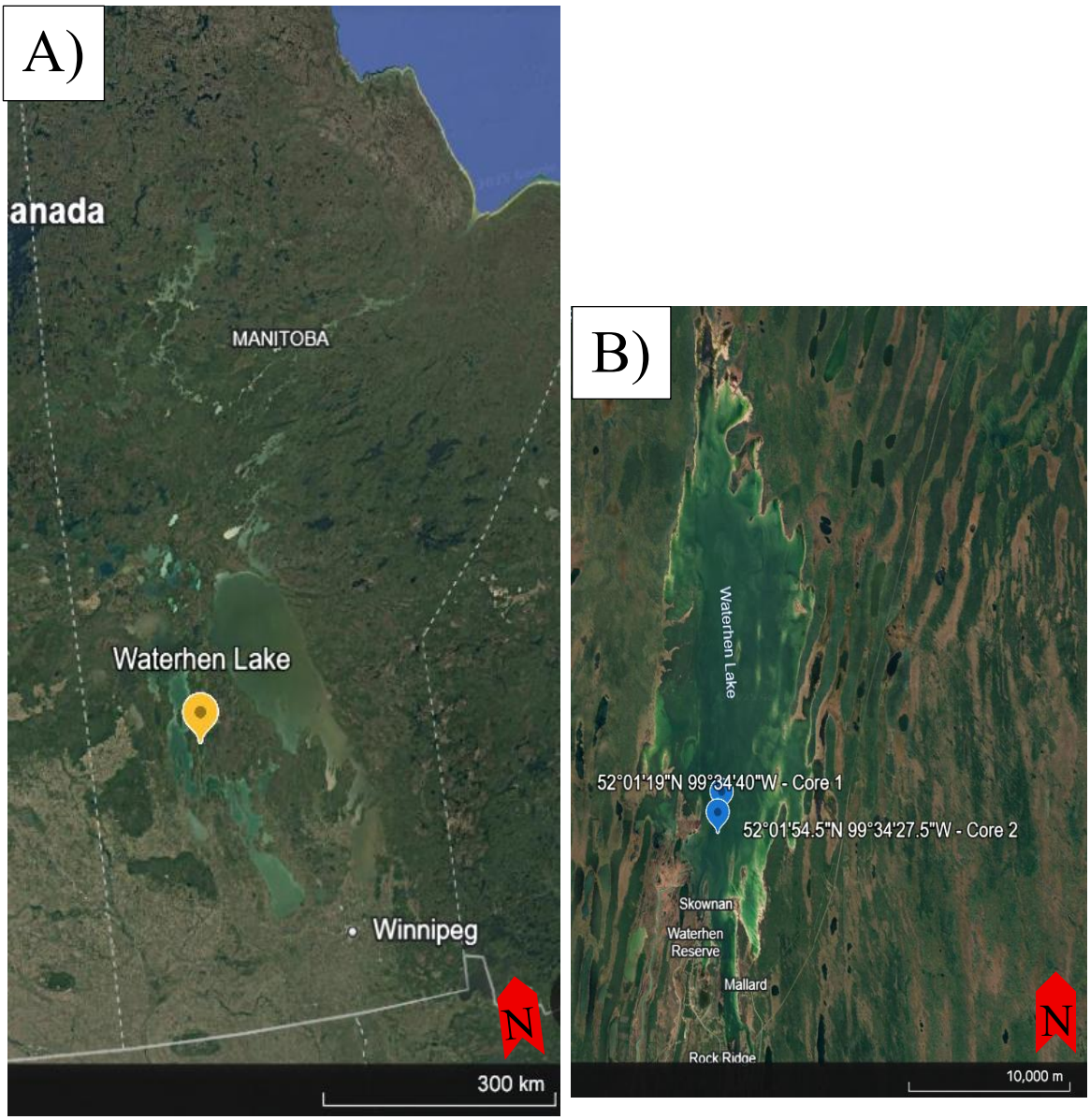



Fig. 2. Lake Waterhen location within the province of Manitoba (panel A) and sediment coring locations in Waterhen Lake (panel B) (Adapted from Google Earth 2025).

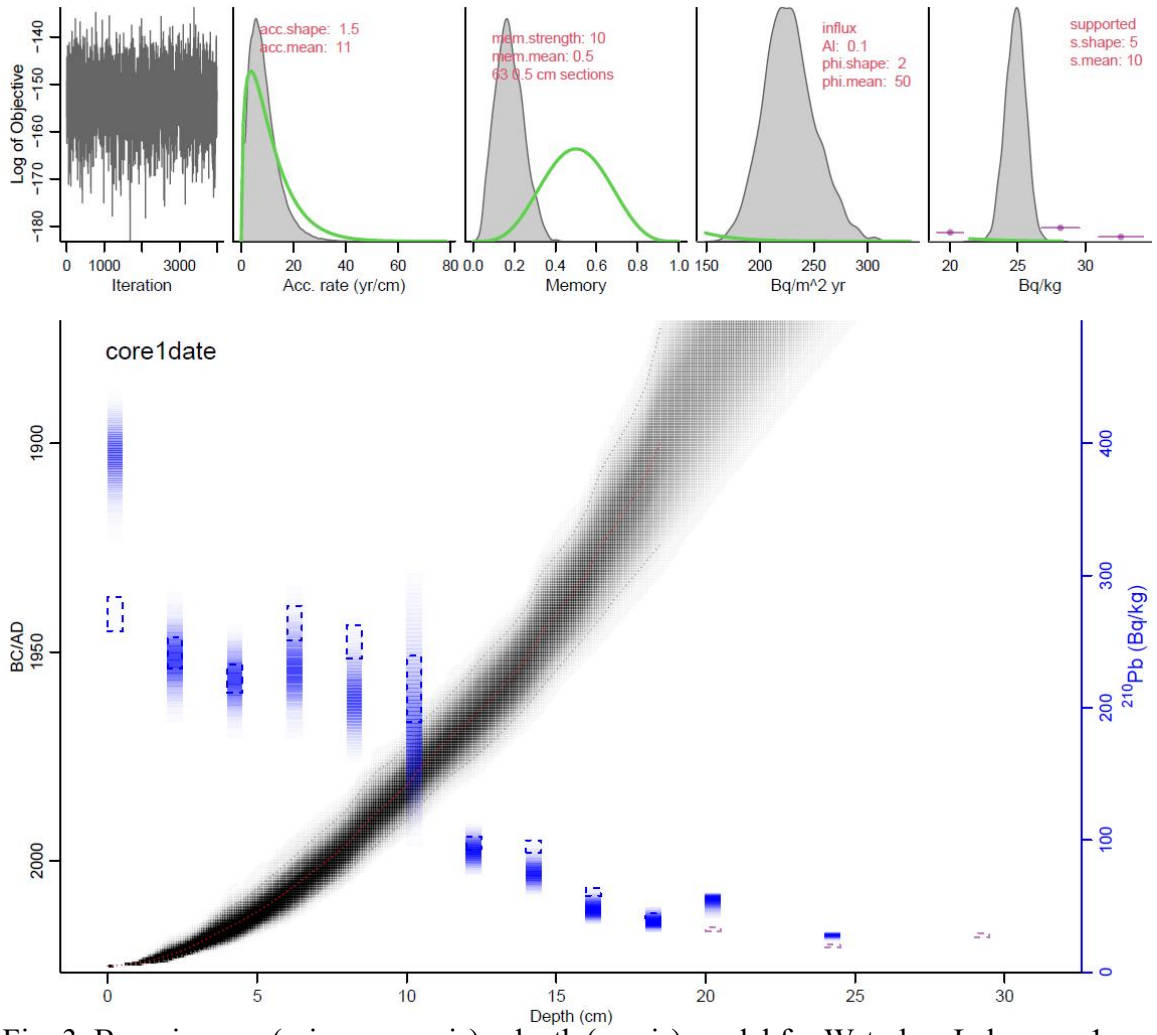



Fig. 3. Bayesian age (primary y-axis) - depth (x axis) model for Waterhen Lake core 1. The estimated date curve is shown in the thin red line with confidence intervals overlain in grey-black shading. The age-depth model produced a basal date of 1900 at 18.5 cm. The secondary y-axis shows $^{210}$Pb activity (Bq/kg) and is displayed by the blue dashed boxes (measured) and blue shaded areas (interpolated). The final three data points are used as measures of background Pb based on $^{226}$Ra results from gamma spectroscopy. Top panels left to right display the number of iterations to build the model, accumulation rate of sediment (mean = 11 yr/cm), accumulation memory, Bq/m$^2$ yr of $^{210}$Pb (mean = 50), and the level of supported $^{210}$Pb.

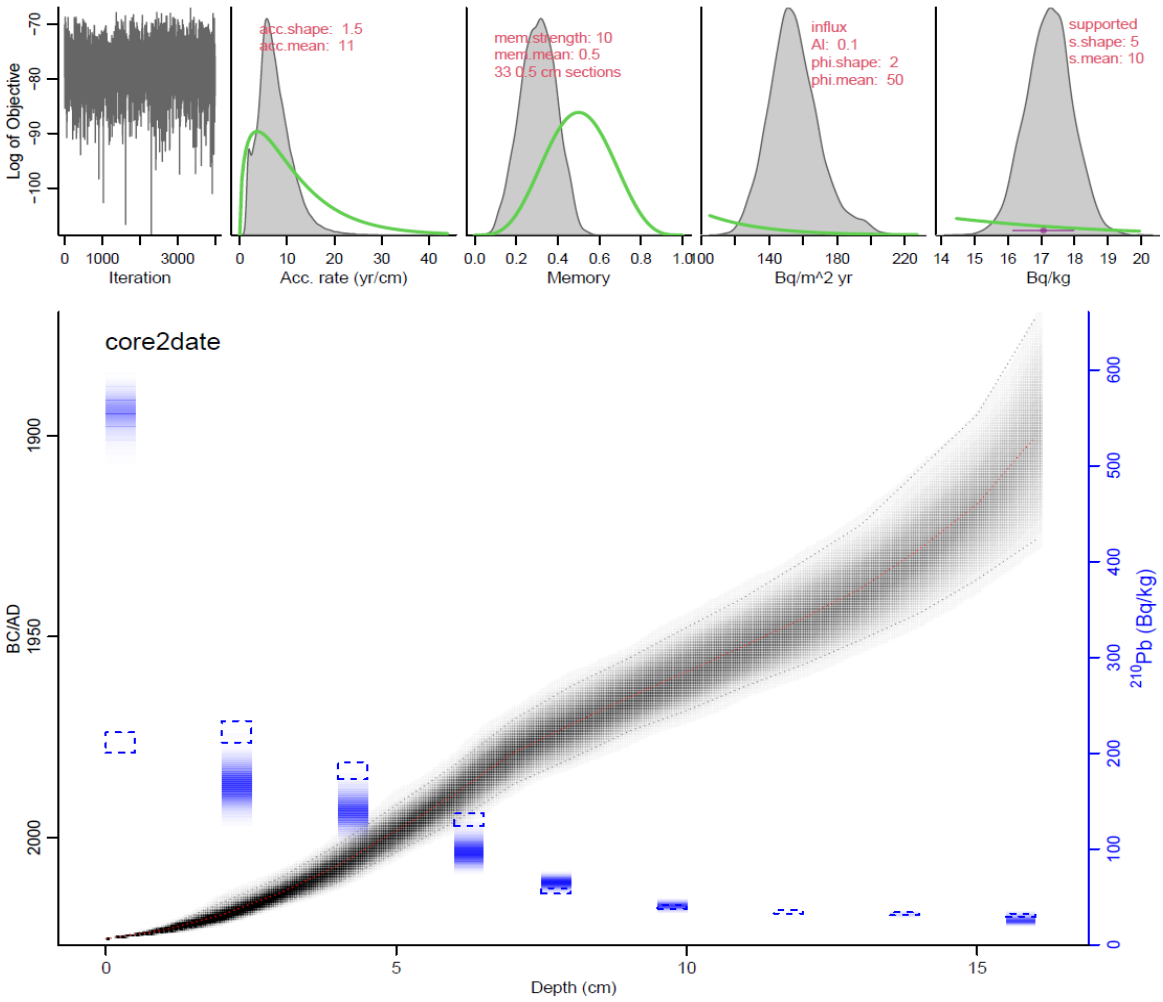



Fig. 4. Bayesian age (primary y-axis) - depth (x axis) model for Waterhen Lake core 2. The estimated date curve is shown in the thin red line with confidence intervals overlain in grey-black shading. The age-depth model produced a basal date of 1900 at 16.0 cm. The secondary y-axis shows $^{210}$Pb activity (Bq/kg) and is displayed by the blue dashed boxes (measured) and blue shaded areas (interpolated). The deepest sediment interval dated (17.5–18.0 cm) was used to set the background $^{210}$Pb activity in this model (not shown on plot). Top panels left to right display the number of iterations to build the model, accumulation rate of sediment (mean = 11 yr/cm), accumulation memory, Bq/m$^2$ yr of $^{210}$Pb (mean = 50), and the level of supported $^{210}$Pb.

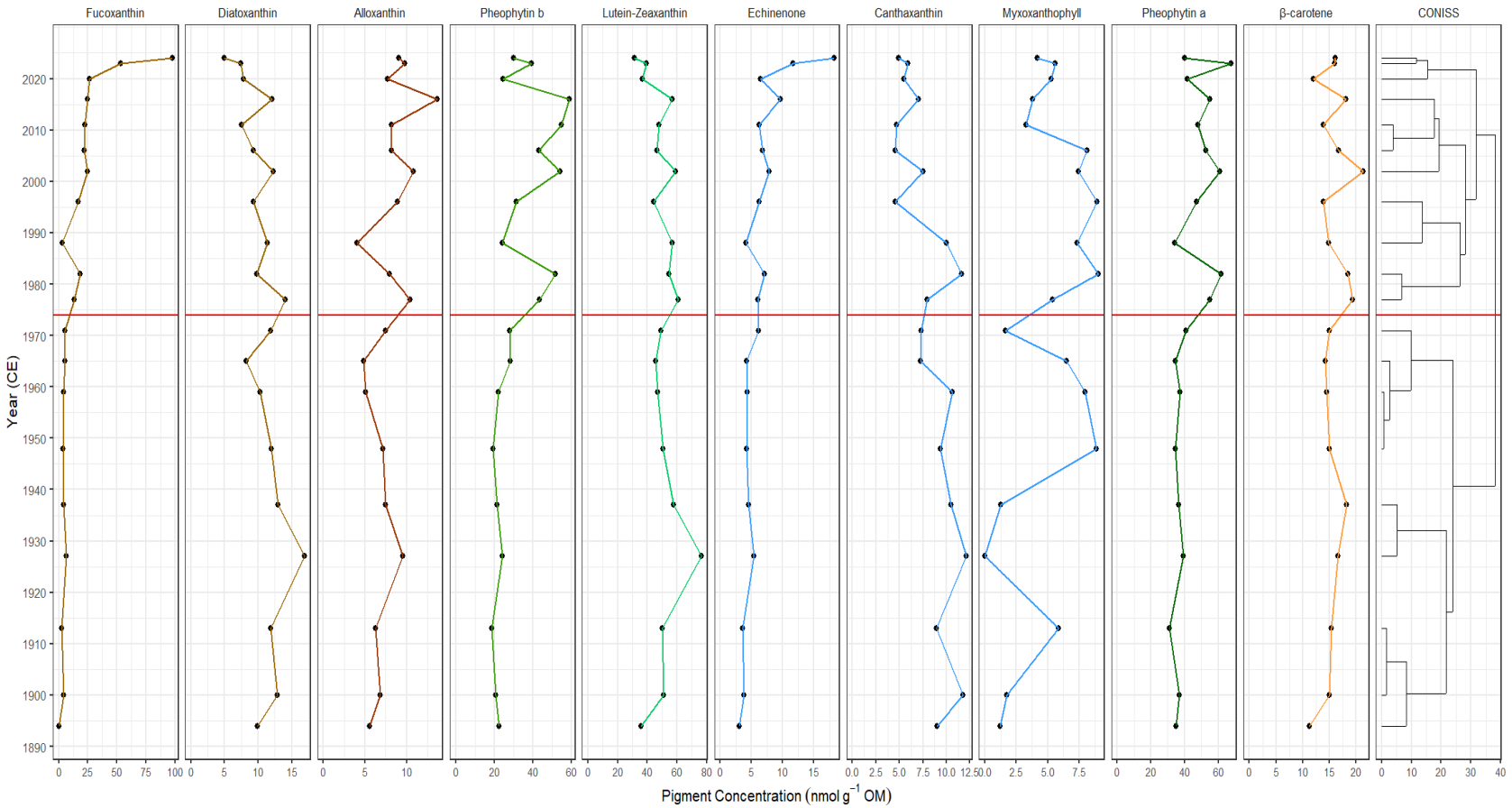

Fucoxanthin
Diatoxanthin
Alloxanthin
Pheophytin b
Lutein-Zeaxanthin
Echinenone
Canthaxanthin
Myxoxanthophyll
Pheophytin a
β-carotene
CONISS
Year (CE)
Pigment Concentration (nmol g$^{-1}$ OM)

Fig. 5. Pigment concentrations (nmol $g^{-1}$ OM) for siliceous algae (fucoxanthin), diatoms (diatoxanthin), cryptophytes (alloxanthin), green algae (pheophytin b), bloom-forming taxa (lutein-zeaxanthin), total cyanobacteria (echinenone), Nostocales cyanobacteria (canthaxanthin), colonial cyanobacteria (myxoxanthophyll), and total algal abundance (pheophytin a and β-carotene) in core 1. Red line represents the significant break between groups as delineated by CONISS analysis validated by a broken stick model (Appendix B, Fig. 6). The x-axis in the CONISS plot is the sum of squares. There are two significant groups (red line = breaks between groups), group one = 1894–1974, group two = 1974–2025. Fucoxanthin was not included in CONISS analysis due to its labile nature (Leavitt, 1993; Leavitt and Hodgeson, 2001).

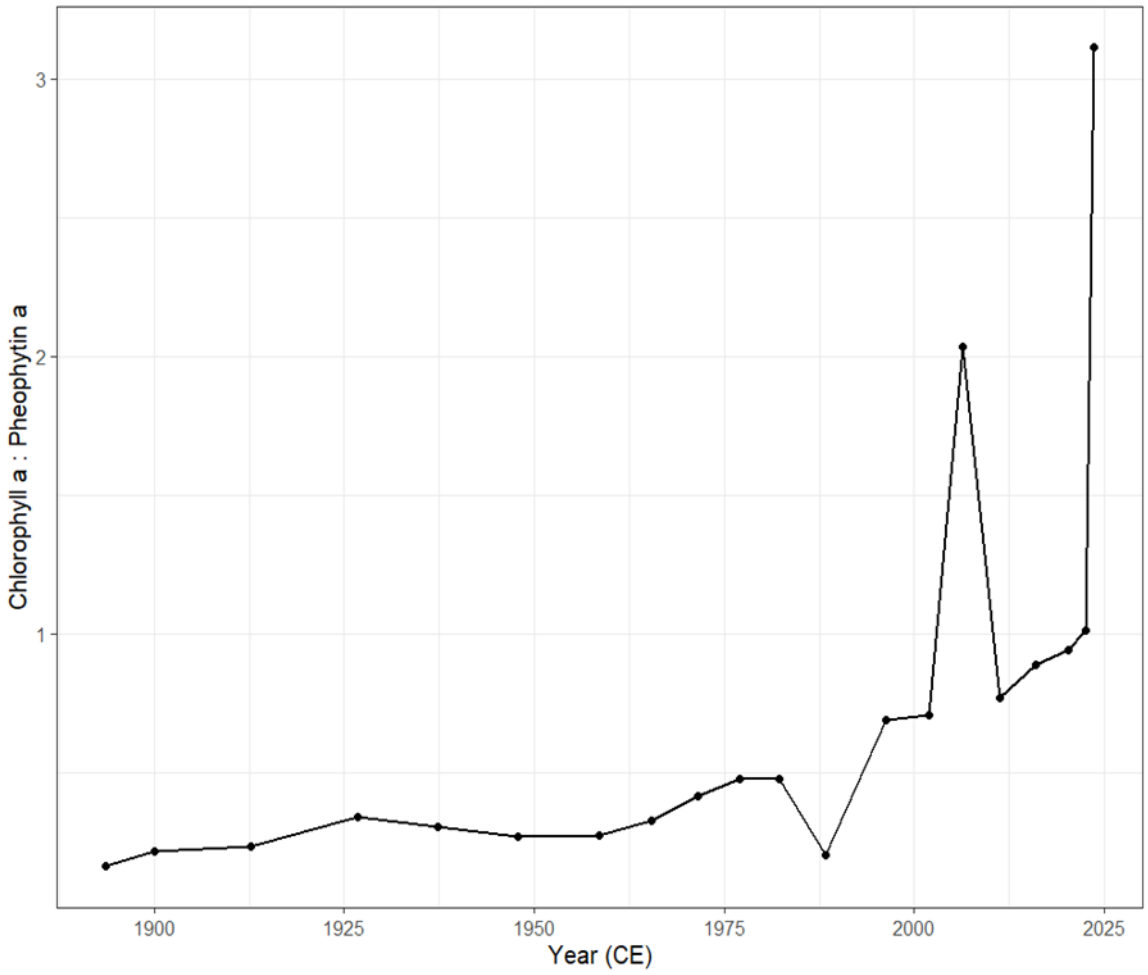



Fig. 6. Chlorophyll a: Pheophytin a ratio plotted by year for core 1 from Waterhen Lake.

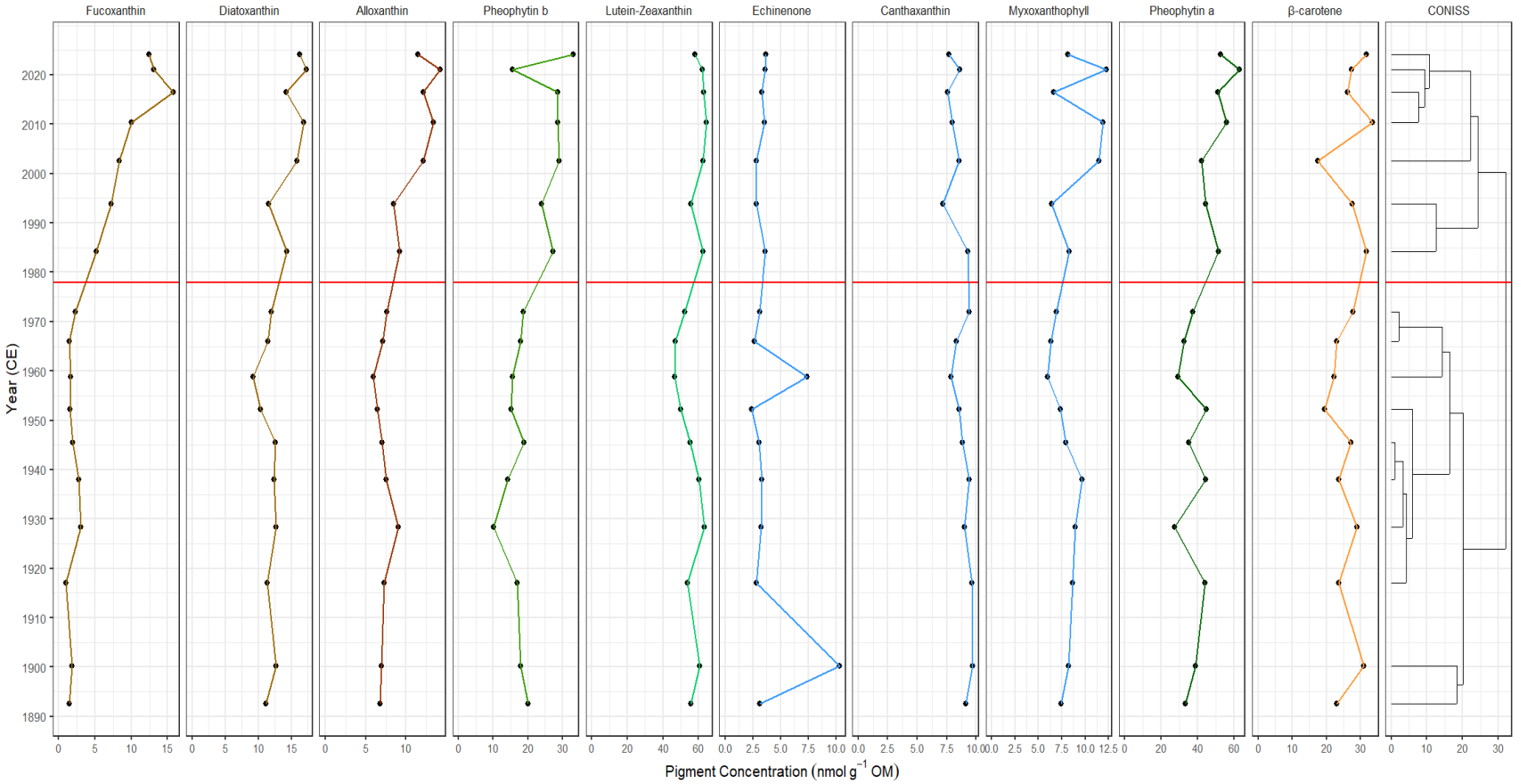

Fucoxanthin
Diatoxanthin
Alloxanthin
Pheophytin b
Lutein-Zeaxanthin
Echinenone
Canthaxanthin
Myxoxanthophyll
Pheophytin a
β-carotene
CONISS
Year (CE)
Pigment Concentration (nmol g$^{-1}$ OM)

Fig. 7. Pigment concentrations (nmol $g^{-1}$ OM) for siliceous algae (fucoxanthin), diatoms (diatoxanthin), cryptophytes (alloxanthin), green algae (pheophytin b), bloom-forming taxa (lutein-zeaxanthin), total cyanobacteria (echinenone), Nostocales cyanobacteria (canthaxanthin), colonial cyanobacteria (myxoxanthophyll), and total algal abundance (pheophytin a and β-carotene) in core 2. Red line represents the significant break between groups as delineated by CONISS analysis (Appendix B, Fig. 7). The x-axis in the CONISS plot is the sum of squares. There are two significant groups (red line = breaks between groups), group one = 1893–1978, group two = 1978–2025. Fucoxanthin was not included in CONISS analysis due to its labile nature (Leavitt, 1993; Leavitt and Hodgeson, 2001).

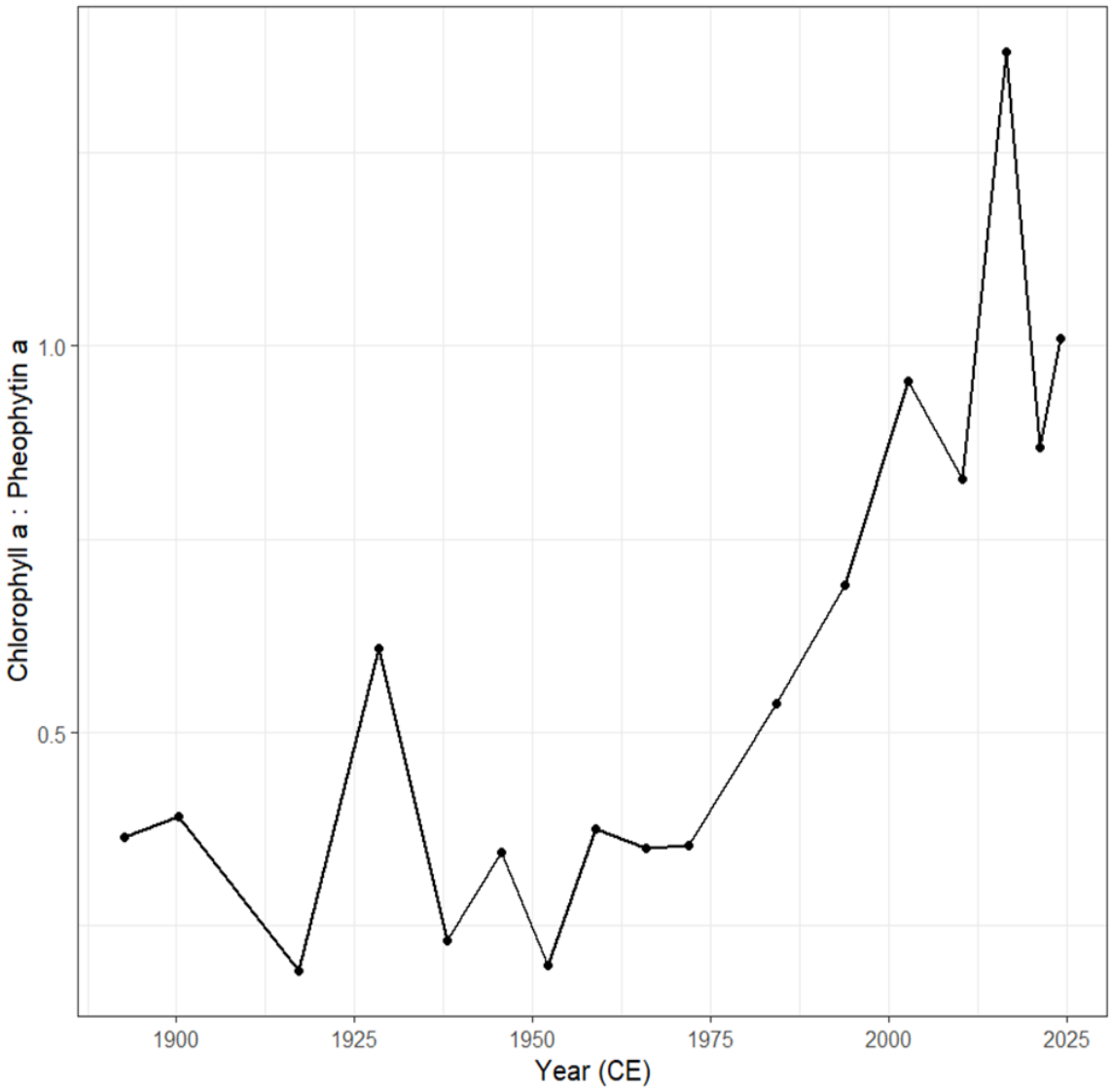



Fig. 8. Chlorophyll a: pheophytin a ratio plotted by year for core 2 from Waterhen Lake.

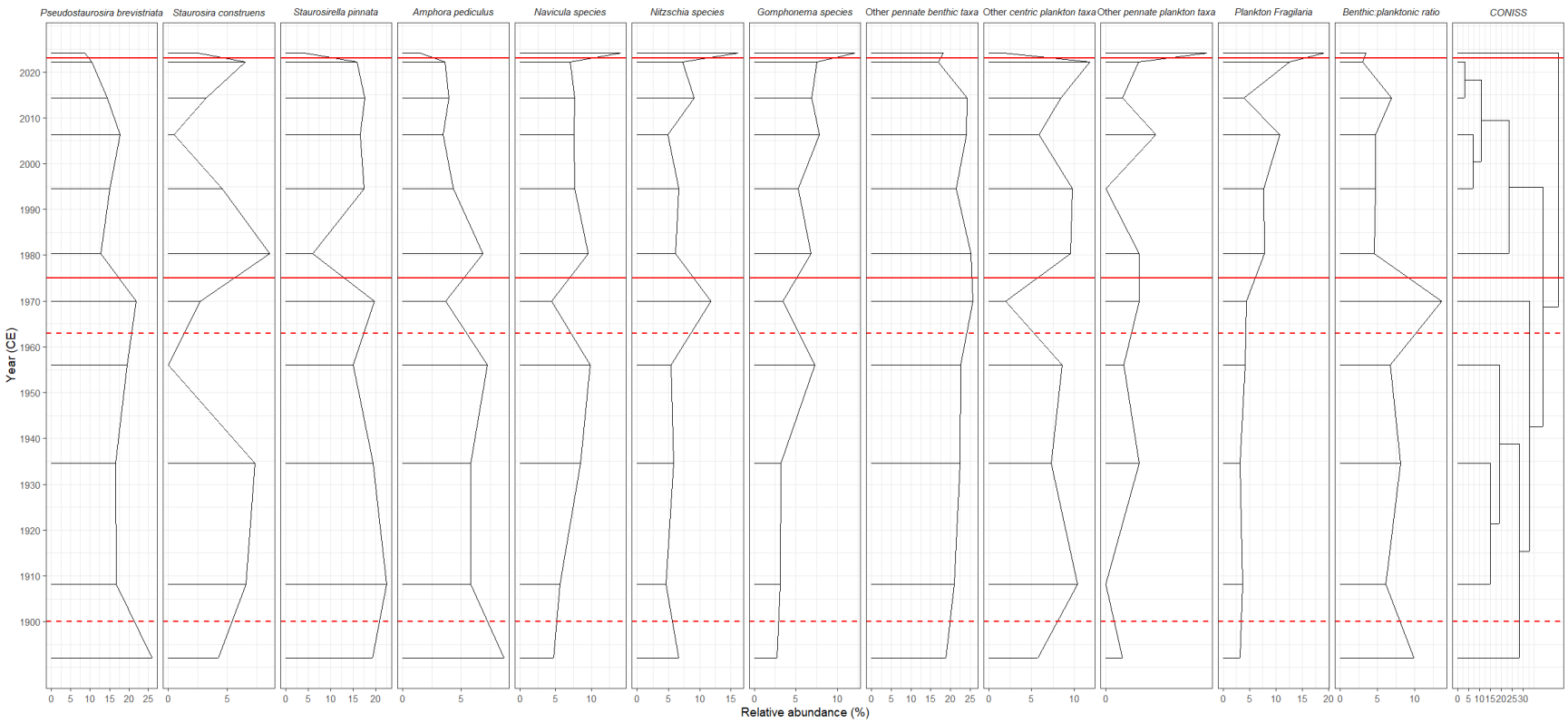

Pseudostaurosira brevistriata
Staurosira construens
Staurosirella pinnata
Amphora pediculus
Navicula species
Nitzschia species
Gomphonema species
Other pennate benthic taxa
Other centric plankton taxa
Other pennate plankton taxa
Plankton Fragilaria
Benthic:planktonic ratio
CONISS
Year (CE)
2020
2010
2000
1990
1980
1970
1960
1950
1940
1930
1920
1910
1900
0 5 10 15 20 25
0 5
0 5 10 15 20
0 5
0 5 10
0 5 10 15
0 5 10
0 5 10 15 20 25
0 5 10
0
0 5 10 15 20
0 5 10
0 5 10 15 20 25 30
Relative abundance (%)

Fig. 9. Diatom relative abundance (%) for core 1. Plot shows 5% relative abundance by Year (CE). CONISS test is for Hellinger transformed 1% relative abundance data by Year (CE). Vertical lines represent significant breaks between groups as delineated by CONISS analysis (solid lines = primary breaks, dashed lines = secondary breaks). The x-axis in the CONISS plot is the sum of squares. There are five significant groupings (group one = 1892–1900, group two = 1900–1963, group three = 1963–1975, group four = 1975–2023, group five = 2023–2025).

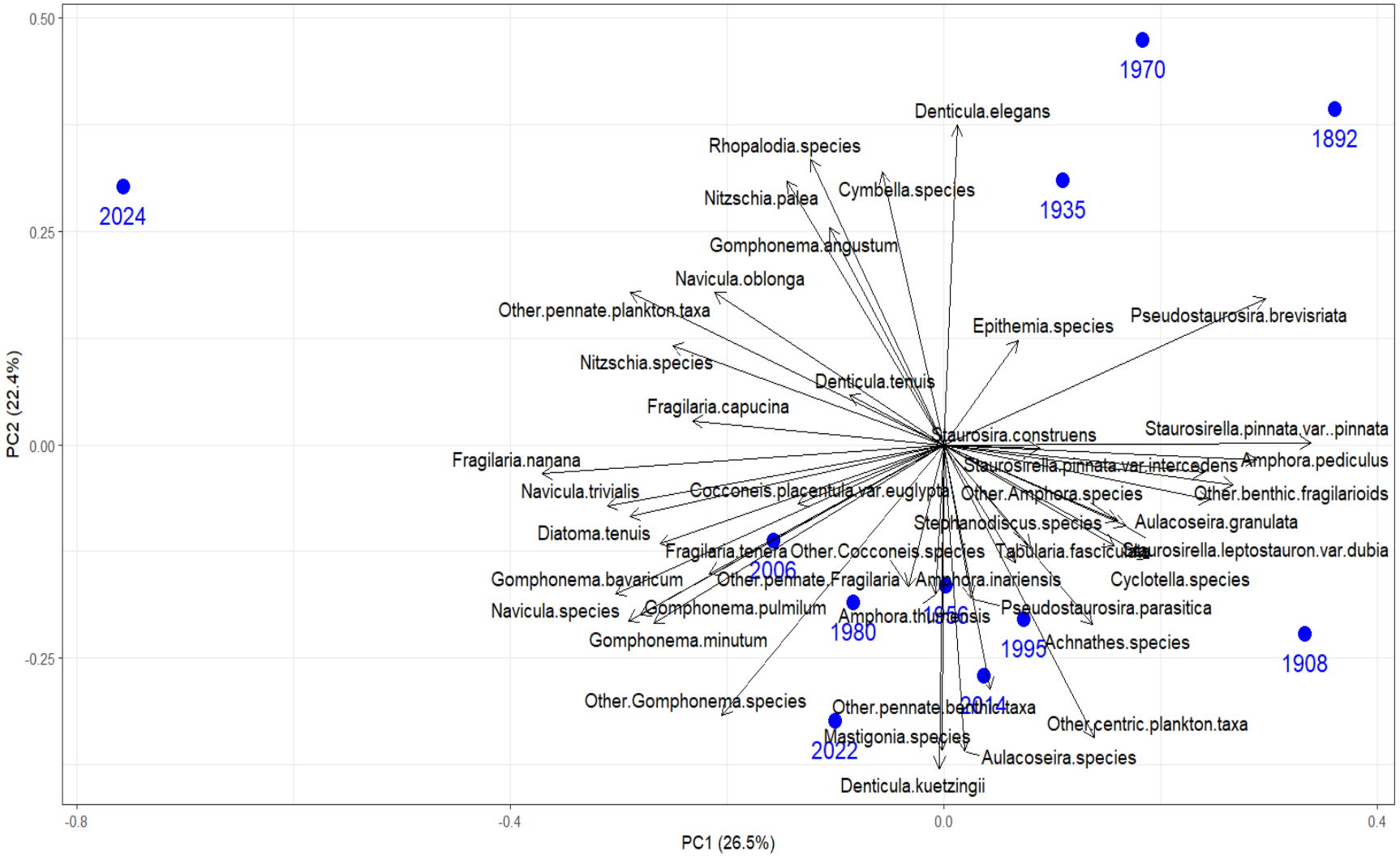

0.50
0.25
0.00
-0.25
PC2 (22.4%)
-0.8
-0.4
0.0
0.4
PC1 (26.5%)
1970
1892
2024
1935
2006
1980
1956
1995
2014
2022
1908
Denticula.elegans
Rhopalodia.species
Nitzschia.palea
Cymbella.species
Gomphonema.angustum
Navicula.oblonga
Other.pennate.plankton.taxa
Epithemia.species
Pseudostaurosira.brevisriata
Nitzschia.species
Denticula.tenuis
Fragilaria.capucina
Staurosira.construens
Staurosirella.pinnata.var..pinnata
Fragilaria.nanana
Staurosirella.pinnata.var.intercedens
Amphora.pediculus
Navicula.trivialis
Cocconeis.placentula.var.euglypta
Other.Amphora.species
Other.benthic.fragilarioids
Stephanodiscus.species
Aulacoseira.granulata
Diatoma.tenuis
Fragilaria.tenera
Other.Cocconeis.species
Tabularia.fasciculata
Staurosirella.leptostauron.var.dubia
Gomphonema.bavaricum
Other.pennate.Fragilaria
Amphora.inariensis
Cyclotella.species
Navicula.species
Gomphonema.pulmilum
Amphora.thumensis
Pseudostaurosira.parasitica
Gomphonema.minutum
Achnathes.species
Other.Gomphonema.species
Other.pennate.benthic.taxa
Other.centric.plankton.taxa
Mastigonia.species
Aulacoseira.species
Denticula.kuetzingii

Fig. 10. PCA analysis plot for Hellinger transformed 1% relative abundance data. PC1 and PC2 explain 48.9% of variability total. PC1 explains 26.5% of the variability and PC2 explains 22.4% of the variability in the data.

**Tables**

Table 1. Core collection information for two sediment cores extracted from Waterhen Lake on March 25, 2025.

| Core Number | Longitude | Latitude | Core length (cm) | Ice Thickness (cm) | Depth (m) |
|---|---|---|---|---|---|
| 1 | 99˚ 34.6730’ | 52˚ 01.3196’ | 35 | 88 | 3.37 |
| 2 | 99˚ 34.4582’ | 52˚ 01.9075’ | 24 | 85 | 2.88 |

**Appendix A – Supplementary Tables**

Table 1. Waterhen Lake water chemistry data from select months in 2016 and 2017. TDN is total dissolved nitrogen, TDP is total dissolved phosphorus, and HPLC chl a is chlorophyll a measured with high performance liquid chromatography. The average TDN: TDP ratio is ~30. Data from C. Hebert, Manitoba Great Lake Program through the Centre for Earth Observational Science (University of Manitoba).

| Year | Month | Day | Latitude | Longitude | TDN (µg/L) | SRP (µg/L) | TDP (µg/L) | HPLC chl a (µg/L) |
|---|---|---|---|---|---|---|---|---|
| 2016 | 5 | 19 | 52.04428 | -99.5703 | 591 | 1 | 5 | 1.34 |
| 2016 | 6 | 9 | 52.04428 | -99.5703 | 697 | 1 | 9 | 2.06 |
| 2016 | 7 | 28 | 52.04428 | -99.5703 | 659 | 1 | 6 | 2.98 |
| 2016 | 8 | 16 | 52.04428 | -99.5703 | 640 | NA | 6 | 2.01 |
| 2016 | 9 | 28 | 52.04428 | -99.5703 | 655 | 6 | 14 | 1.51 |
| 2017 | 4 | 12 | 52.04428 | -99.5703 | NA | NA | NA | 1.06 |
| 2017 | 5 | 20 | 52.04428 | -99.5703 | 557 | 1 | 5 | 1.39 |
| 2017 | 8 | 4 | 52.04428 | -99.5703 | 655 | 93 | 102 | 2.2 |
| 2017 | 9 | 17 | 52.04428 | -99.5703 | 637 | 6 | 12 | 2.77 |
| 2017 | 10 | 5 | 52.04428 | -99.5703 | 611 | 29 | 34 | 1.7 |
| 2017 | 10 | 17 | 52.04428 | -99.5703 | 605 | 9 | 14 | 1.82 |
| Mean | NA | NA | NA | NA | 631 | 16.3 | 20.7 | 1.89 |

## Appendix B – Supplimentary Figures

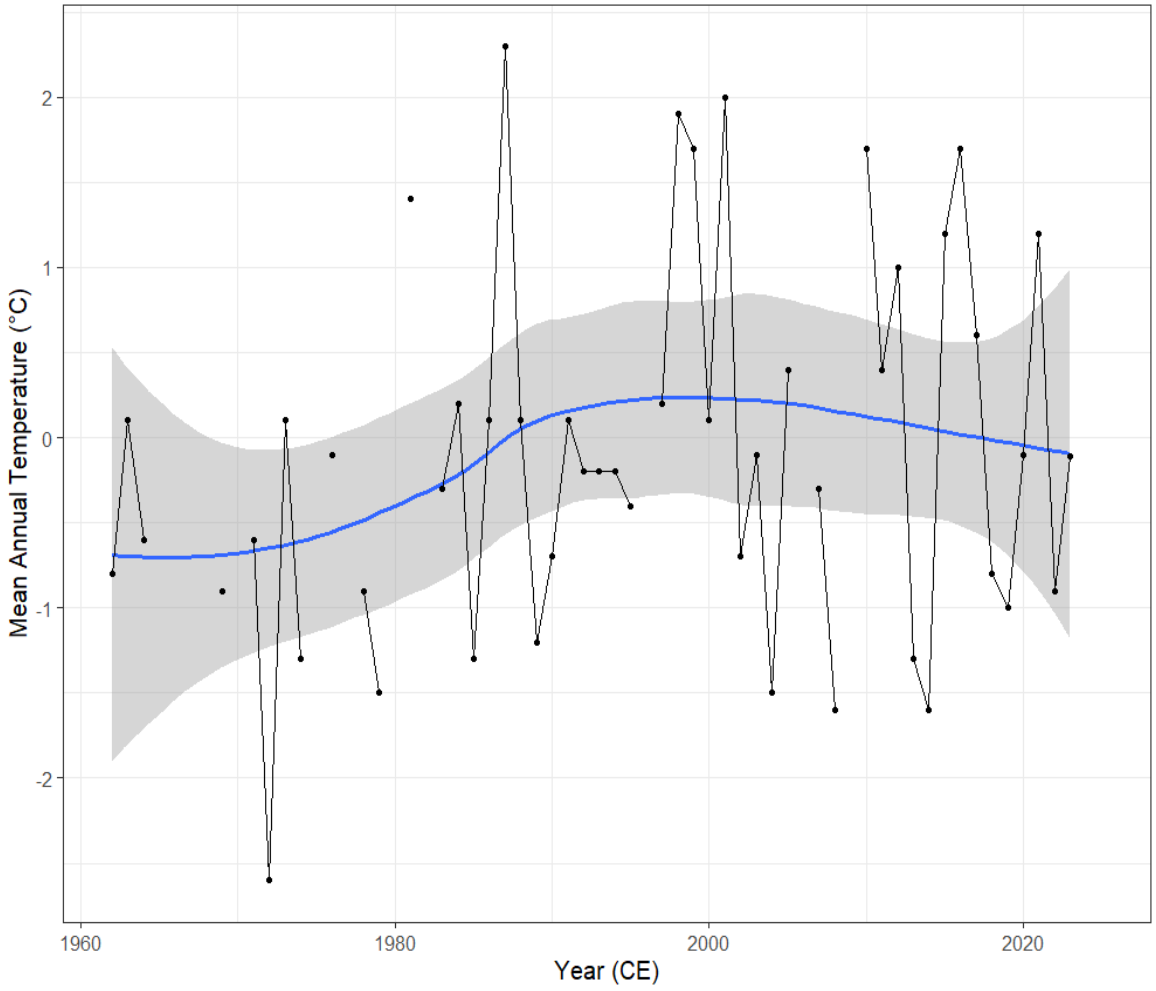



Fig. 1. Long-term (~1960–2023) mean annual temperature (˚C) climate data from Grand Rapids, Manitoba (ECCC 2025b). The blue line is the locally weighted scatterplot smoothing (LOESS) line and the grey area is the 95% confidence interval.

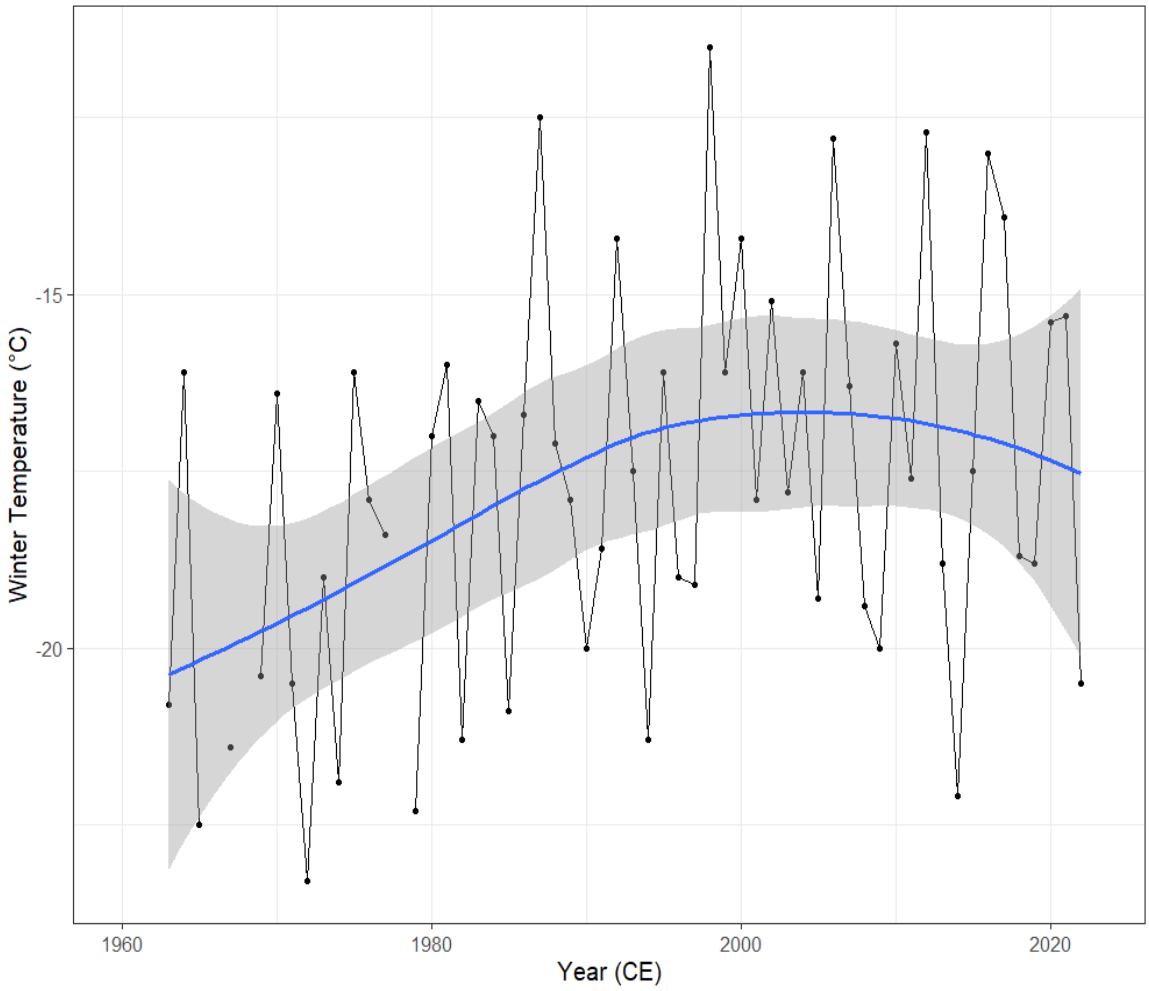



Fig. 2. Long-term (~1960–2023) mean winter temperature (˚C) climate data from Grand Rapids, Manitoba (ECCC 2025b). The blue line is the locally weighted scatterplot smoothing (LOESS) line and the grey area is the 95% confidence interval.

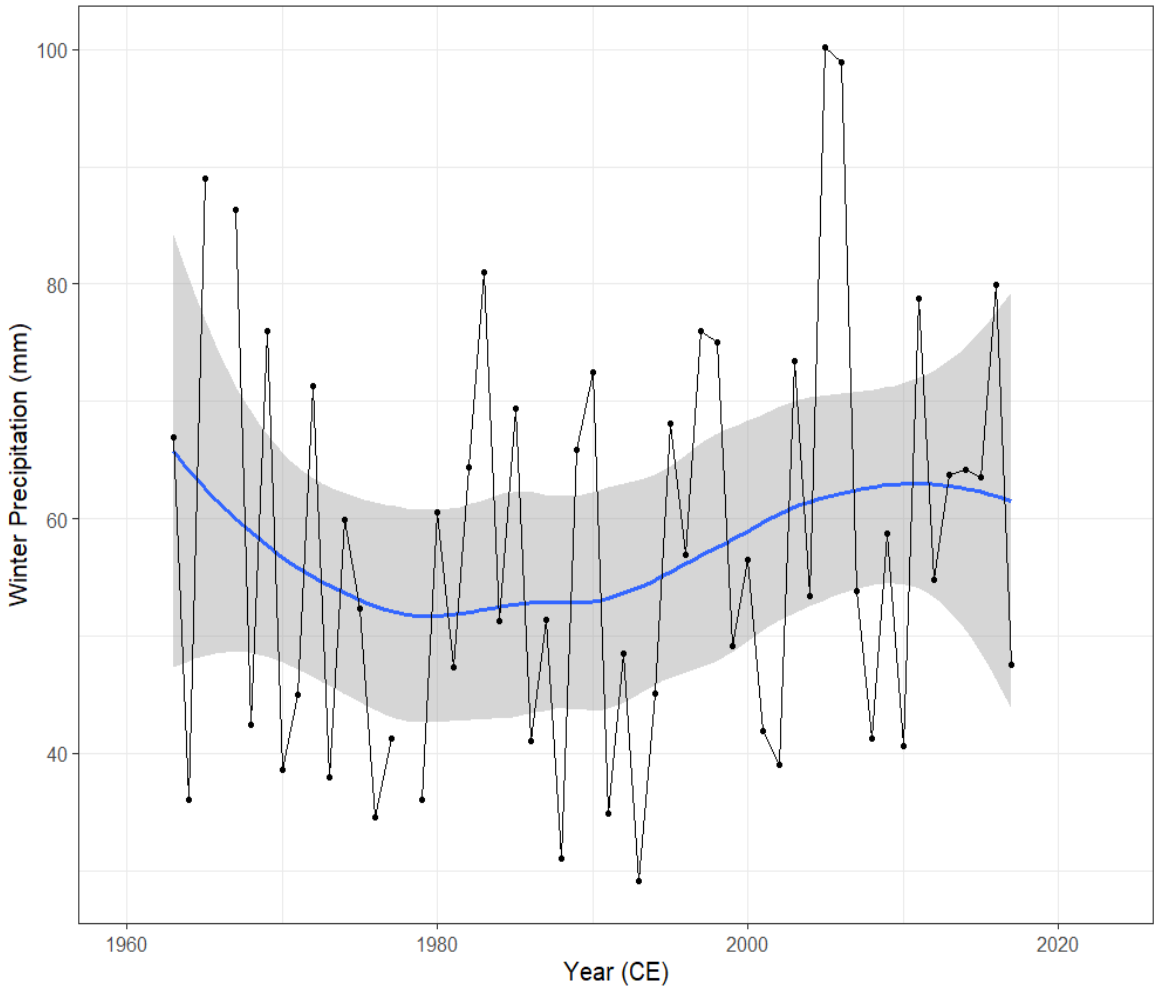



Fig. 3. Long-term (~1960–2017) mean winter precipitation (mm) climate data from Grand Rapids, Manitoba (ECCC 2025a). The blue line is the locally weighted scatterplot smoothing (LOESS) line and the grey area is the 95% confidence interval.

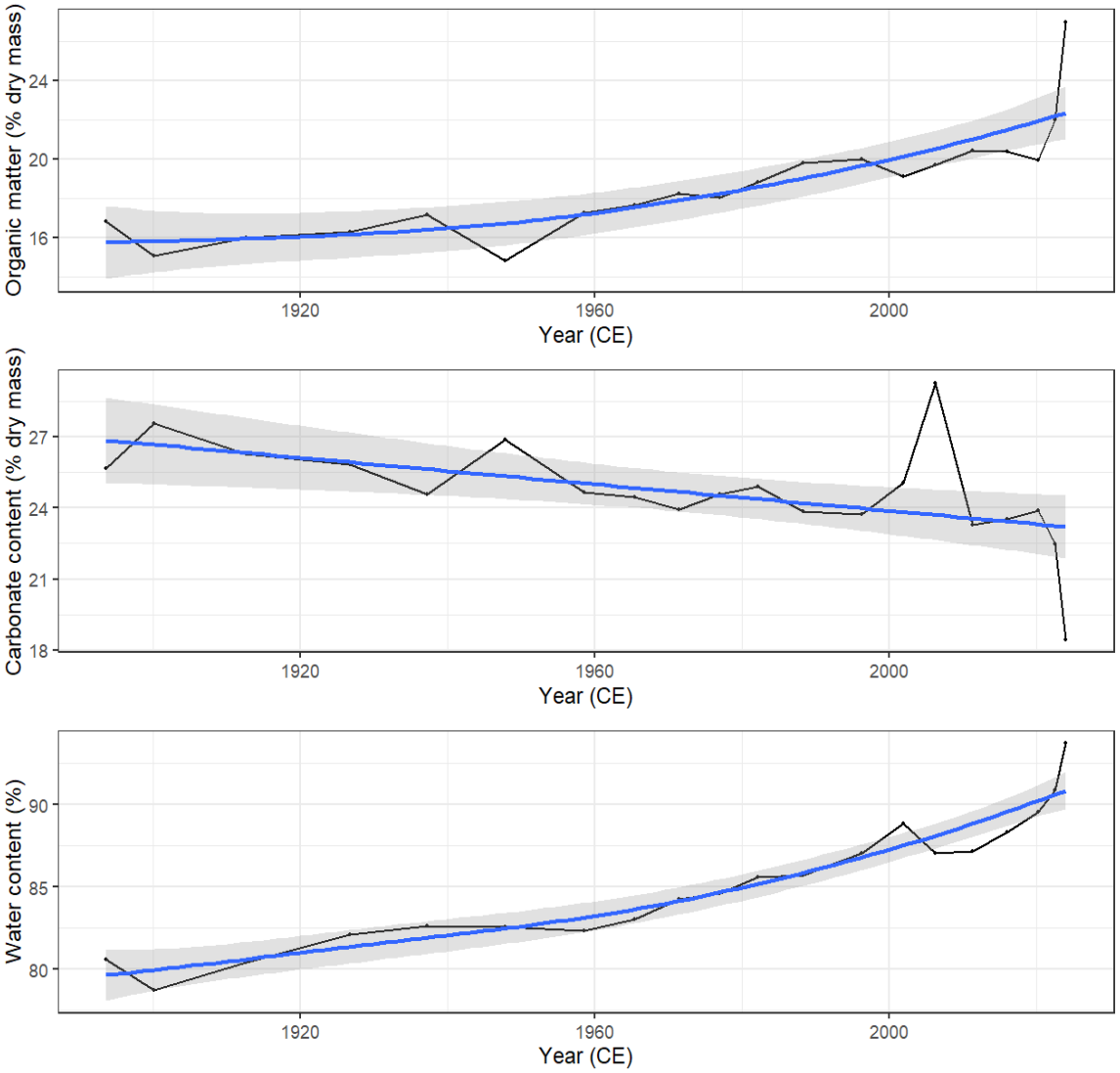



Fig. 4. LOI results for core 1, showing water content (%), organic matter (% dry mass), and carbonate content (% dry mass). The blue line is the generalized additive model (GAM) smoothing line and the grey area is the 95% confidence interval.

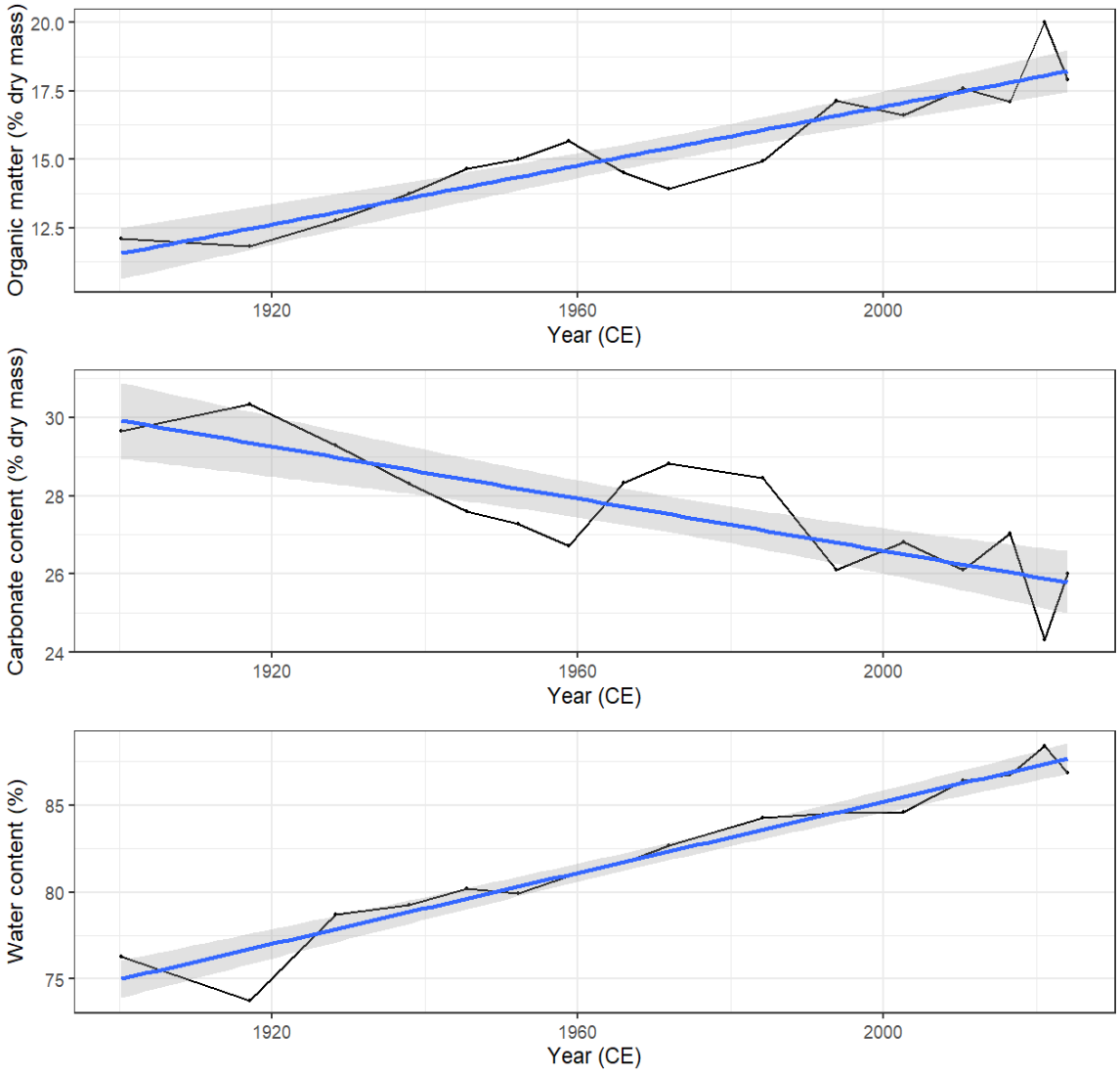



Fig. 5. LOI results for core 2, showing water content (%), organic matter (% dry mass), and carbonate content (% dry mass). The blue line is the generalized additive model (GAM) smoothing line and the grey area is the 95% confidence interval.

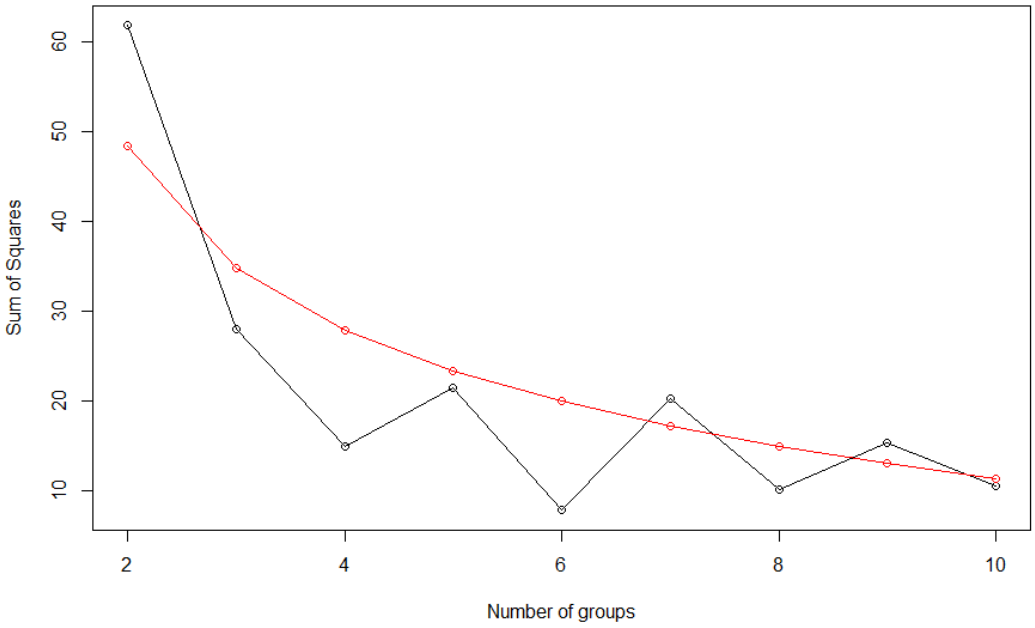



Fig. 6. Broken stick model for core 1 pigments, showing two significant groups (number of groups on the y-axis before the lines intersect).

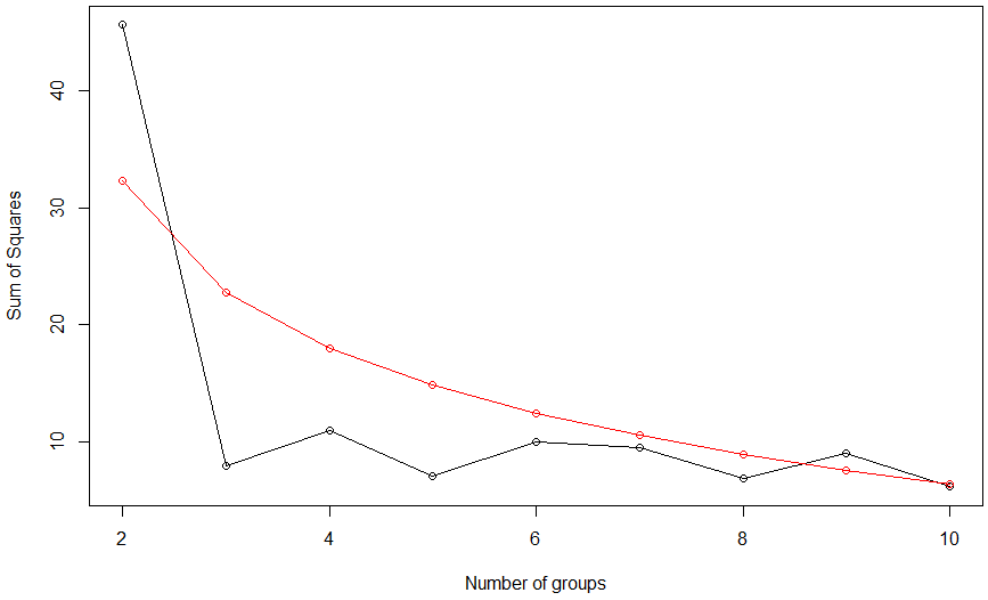



Fig. 7. Broken stick model for core 2 pigments, showing two significant groups (number of groups on the y-axis before the lines intersect).

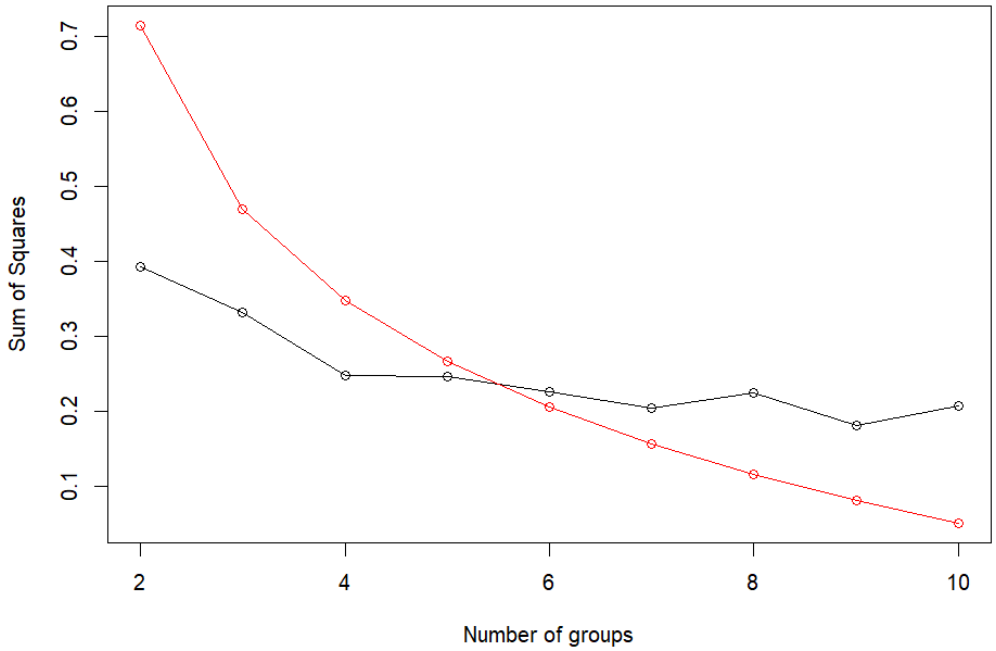



Fig. 8. Broken stick model for core 1 1% diatom relative abundance, showing five significant groups (number of groups on the y-axis before the lines intersect).

**Appendix C – Core Data**

Table 1. Type of analysis per 0.5-cm interval in core 1. Bolded LOI intervals were plotted. Bolded pigment analysis intervals were included in plotting and statistical analysis. Bolded diatom analysis intervals had valves enumerated and identified and were used in plotting and statistical analysis.

| Section Start (cm) | Section End (cm) | Mid depth (cm) | Dating analysis | LOI | Pigment analysis | Diatom analysis |
|---|---|---|---|---|---|---|
| 0.00 | 0.50 | 0.25 | X | | | **X** |
| 0.50 | 1.00 | 0.75 | | **X** | **X** | |
| 1.00 | 1.50 | 1.25 | | | | X |
| 1.50 | 2.00 | 1.75 | | **X** | **X** | |
| 2.00 | 2.50 | 2.25 | X | | | **X** |
| 2.50 | 3.00 | 2.75 | | **X** | **X** | |
| 3.00 | 3.50 | 3.25 | | | | X |
| 3.50 | 4.00 | 3.75 | | **X** | **X** | |
| 4.00 | 4.50 | 4.25 | X | | | **X** |
| 4.50 | 5.00 | 4.75 | | **X** | **X** | |
| 5.00 | 5.50 | 5.25 | | | | X |
| 5.50 | 6.00 | 5.75 | | **X** | **X** | |
| 6.00 | 6.50 | 6.25 | X | | | **X** |
| 6.50 | 7.00 | 6.75 | | **X** | **X** | |
| 7.00 | 7.50 | 7.25 | | | | X |

| | | | | | | |
|---|---|---|---|---|---|---|
| 7.50 | 8.00 | 7.75 | | **X** | **X** | |
| 8.00 | 8.50 | 8.25 | X | | | **X** |
| 8.50 | 9.00 | 8.75 | | **X** | **X** | |
| 9.00 | 9.50 | 9.25 | | | | X |
| 9.50 | 10.00 | 9.75 | | **X** | **X** | |
| 10.00 | 10.50 | 10.25 | X | | | **X** |
| 10.50 | 11.00 | 10.75 | | **X** | **X** | |
| 11.00 | 11.50 | 11.25 | | | | X |
| 11.50 | 12.00 | 11.75 | | **X** | **X** | |
| 12.00 | 12.50 | 12.25 | X | | | **X** |
| 12.50 | 13.00 | 12.75 | | **X** | **X** | |
| 13.00 | 13.50 | 13.25 | | | | X |
| 13.50 | 14.00 | 13.75 | | **X** | **X** | |
| 14.00 | 14.50 | 14.25 | X | | | **X** |
| 14.50 | 15.00 | 14.75 | | **X** | **X** | |
| 15.00 | 15.50 | 15.25 | | | | X |
| 15.50 | 16.00 | 15.75 | | **X** | **X** | |
| 16.00 | 16.50 | 16.25 | X | | | **X** |
| 16.50 | 17.00 | 16.75 | | **X** | **X** | |
| 17.00 | 17.50 | 17.25 | | | | X |
| 17.50 | 18.00 | 17.75 | | **X** | **X** | |
| 18.00 | 18.50 | 18.25 | X | | | **X** |
| 18.50 | 19.00 | 18.75 | | **X** | **X** | |

| | | | | | | |
|---|---|---|---|---|---|---|
| 19.00 | 19.50 | 19.25 | | | | X |
| 19.50 | 20.00 | 19.75 | | **X** | **X** | |
| 20.00 | 20.50 | 20.25 | X | | | **X** |
| 20.50 | 21.00 | 20.75 | | X | X | |
| 21.00 | 21.50 | 21.25 | | | | X |
| 21.50 | 22.00 | 21.75 | | X | X | |
| 22.00 | 22.50 | 22.25 | | | | X |
| 22.50 | 23.00 | 22.75 | | X | X | |
| 23.00 | 23.50 | 23.25 | | | | X |
| 23.50 | 24.00 | 23.75 | | X | X | |
| 24.00 | 24.50 | 24.25 | X | | | X |
| 24.50 | 25.00 | 24.75 | | X | X | |
| 25.00 | 25.50 | 25.25 | | | | X |
| 25.50 | 26.00 | 25.75 | | X | X | |
| 26.00 | 26.50 | 26.25 | | | | X |
| 26.50 | 27.00 | 26.75 | | X | X | |
| 27.00 | 27.50 | 27.25 | | | | X |
| 27.50 | 28.00 | 27.75 | | X | X | |
| 28.00 | 28.50 | 28.25 | | | | X |
| 28.50 | 29.00 | 28.75 | | X | X | |
| 29.00 | 29.50 | 29.25 | X | | | X |
| 29.50 | 30.00 | 29.75 | | X | X | |
| 30.00 | 30.50 | 30.25 | | | | X |

Table 2. Type of analysis per 0.5-cm interval in core 2.

| Section Start (cm) | Section End (cm) | Mid depth (cm) | Date analysis | LOI | Pigment analysis |
|---|---|---|---|---|---|
| 0.0 | 0.5 | 0.25 | X | | |
| 0.5 | 1.0 | 0.75 | | X | X |
| 1.0 | 1.5 | 1.25 | | | |
| 1.5 | 2.0 | 1.75 | | X | X |
| 2.0 | 2.5 | 2.25 | X | | |
| 2.5 | 3.0 | 2.75 | | X | X |
| 3.0 | 3.5 | 3.25 | | | |
| 3.5 | 4.0 | 3.75 | | X | X |
| 4.0 | 4.5 | 4.25 | X | | |
| 4.5 | 5.0 | 4.75 | | X | X |
| 5.0 | 5.5 | 5.25 | | | |
| 5.5 | 6.0 | 5.75 | | X | X |
| 6.0 | 6.5 | 6.25 | X | | |
| 6.5 | 7.0 | 6.75 | | X | X |
| 7.0 | 7.5 | 7.25 | | | |
| 7.5 | 8.0 | 7.75 | X | | |
| 8.0 | 8.5 | 8.25 | | X | X |
| 8.5 | 9.0 | 8.75 | | | |

| | | | | | |
|---|---|---|---|---|---|
| 9.0 | 9.5 | 9.25 | | X | X |
| 9.5 | 10.0 | 9.75 | X | | |
| 10.0 | 10.5 | 10.25 | | X | X |
| 10.5 | 11.0 | 10.75 | | | |
| 11.0 | 11.5 | 11.25 | | X | X |
| 11.5 | 12.0 | 11.75 | X | | |
| 12.0 | 12.5 | 12.25 | | X | X |
| 12.5 | 13.0 | 12.75 | | | |
| 13.0 | 13.5 | 13.25 | | X | X |
| 13.5 | 14.0 | 13.75 | X | | |
| 14.0 | 14.5 | 14.25 | | X | X |
| 14.5 | 15.0 | 14.75 | | | |
| 15.0 | 15.5 | 15.25 | | X | X |
| 15.5 | 16.0 | 15.75 | X | | |
| 16.0 | 16.5 | 16.25 | | X | X |
| 16.5 | 17.0 | 16.75 | | | |
| 17.0 | 17.5 | 17.25 | | X | X |
| 17.5 | 18.0 | 17.75 | X | | |

## Appendix D – Calculations

### Dating Calculations

Equation 1

$^{210}$Pb activity = [Activity ($^{209}$Po spike) * $^{210}$Po counts] / [mass (g) * $^{209}$Po counts * e^(-0.00501*days after plating)] – [0.0012 / mass (g)]

Formula from Eakins and Morrison (1978).

### LOI Calculations

Equation 2

Organic matter = LOI 550 = ((DW105 - DW550) / DW105) * 100

Equation 3

Carbonate content = LOI 950 = ((DW550 – DW950) / DW105) * 100

DW = Dry weight

Formulas from Heiri et al. (2001).